

Insights on the $Z_b(10610)$ and $Z_b(10650)$ from the dipion decays

Vadim Baru

Institut für Theoretische Physik II, Ruhr-Universität Bochum Germany

ITEP, Moscow, Russia

EMMI Workshop

Experimental and theoretical status of and perspectives for XYZ states

12-15 April 2021

based on

VB, E.Epelbaum, A.A.Filin, C.Hanhart, R.V.Mizuk, A.Nefediev, and S.Ropertz

Phys. Rev. D 103, 034016 (2021)

$Z_b(10610)$ and $Z_b(10650)$ from $\Upsilon(10860)$ decays at Belle

$$\Upsilon(10860) \rightarrow \pi\pi\Upsilon(nS), \quad n = 1, 2, 3$$

$$\Upsilon(10860) \rightarrow \pi\pi h_b(mP), \quad m = 1, 2$$

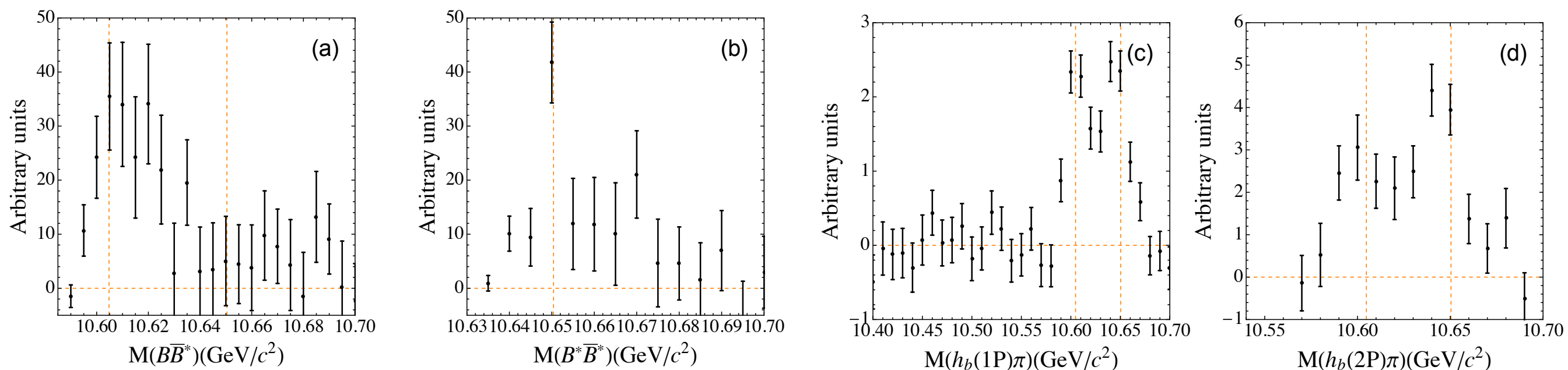
$$\Upsilon(10860) \rightarrow \pi B^{(*)} \bar{B}^*$$

Bondar et al. PRL108, 122001(2012)

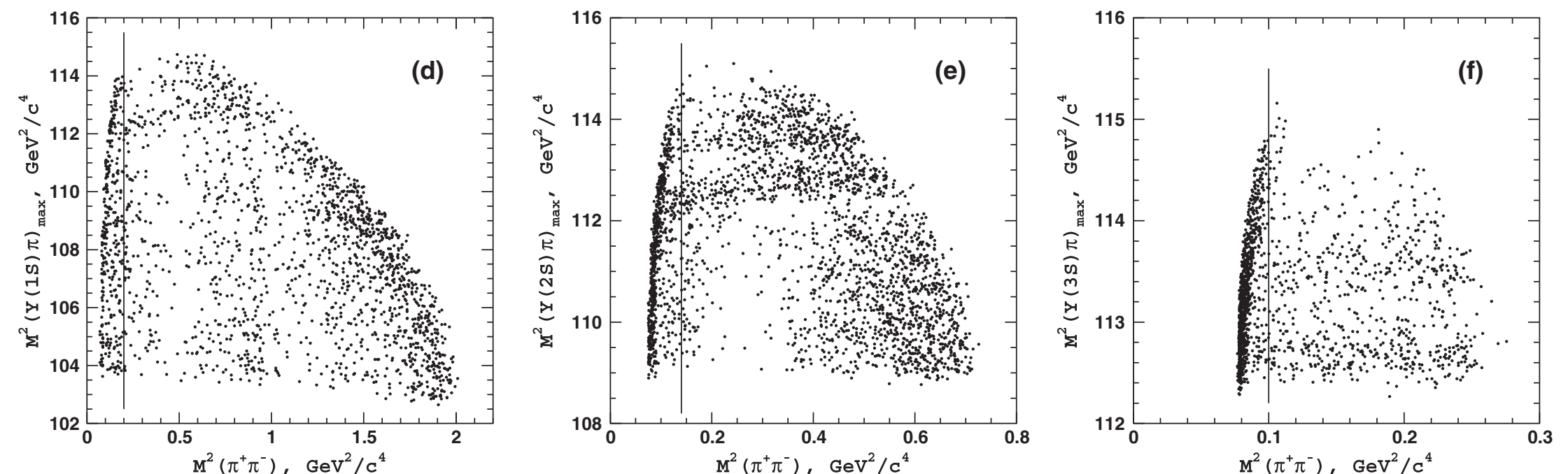
Garmash et al. PRL116, 212001(2016)

PRD91, 072003 (2015)

- Invariant mass distributions in BB^* , B^*B^* and $h_b(mP)\pi$ channels



- Dalitz plots for $\Upsilon(10860) \rightarrow \pi\pi\Upsilon(nS)$ and its projections to $\Upsilon(nS)\pi$ and $\pi\pi$



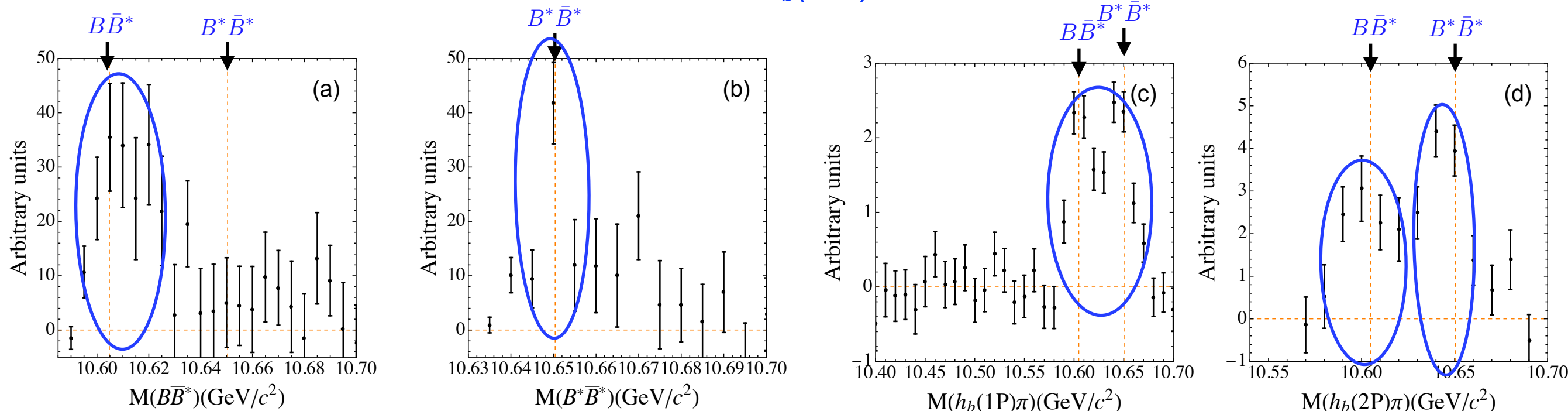
$Z_b(10610)$ and $Z_b(10650)$ from $\Upsilon(10860)$ decays at Belle

$$\Upsilon(10860) \rightarrow \pi\pi\Upsilon(nS), \quad n = 1, 2, 3$$

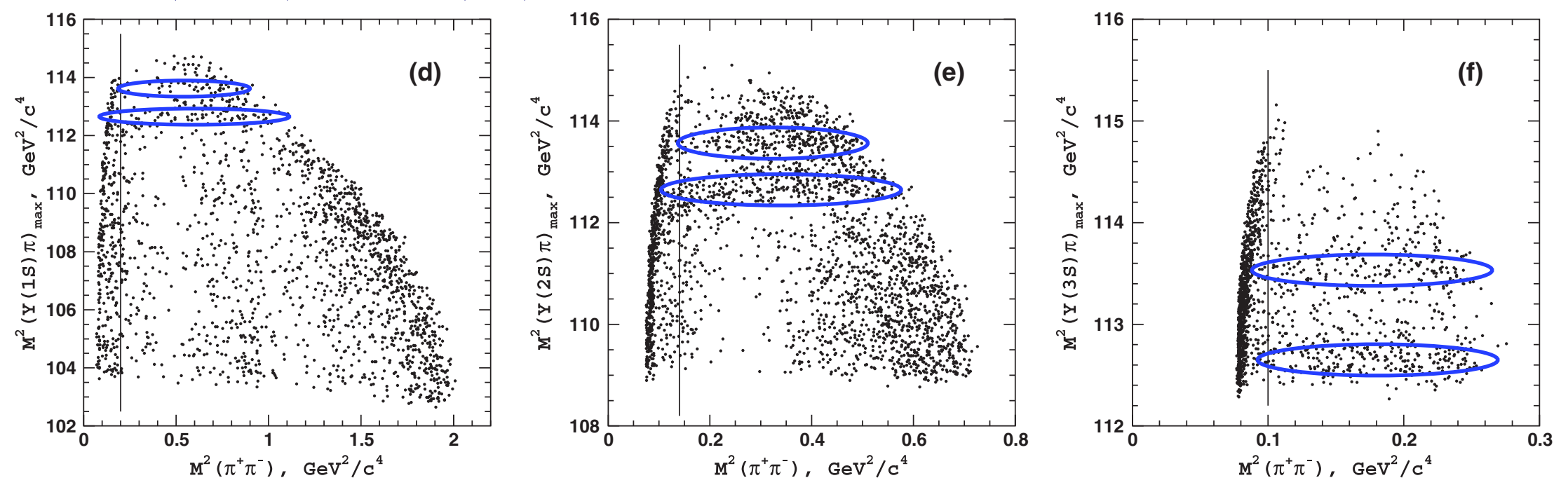
$$\Upsilon(10860) \rightarrow \pi\pi h_b(mP), \quad m = 1, 2$$

$$\Upsilon(10860) \rightarrow \pi B^{(*)} \bar{B}^*$$

- Invariant mass distributions in BB^* , B^*B^* and $h_b(mP)\pi$ channels



- Dalitz plot for $\Upsilon(10860) \rightarrow \pi\pi\Upsilon(nS)$ and its projections to $\Upsilon(nS)\pi$ and $\pi\pi$



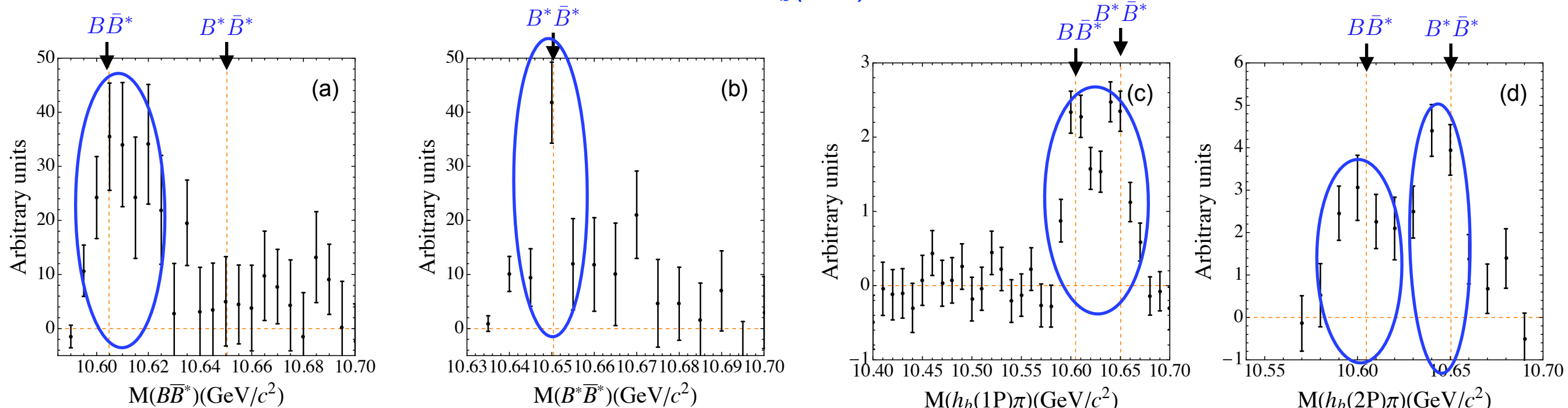
$Z_b(10610)$ and $Z_b(10650)$ from $\Upsilon(10860)$ decays at Belle

$$\Upsilon(10860) \rightarrow \pi\pi\Upsilon(nS), \quad n = 1, 2, 3$$

$$\Upsilon(10860) \rightarrow \pi\pi h_b(mP), \quad m = 1, 2$$

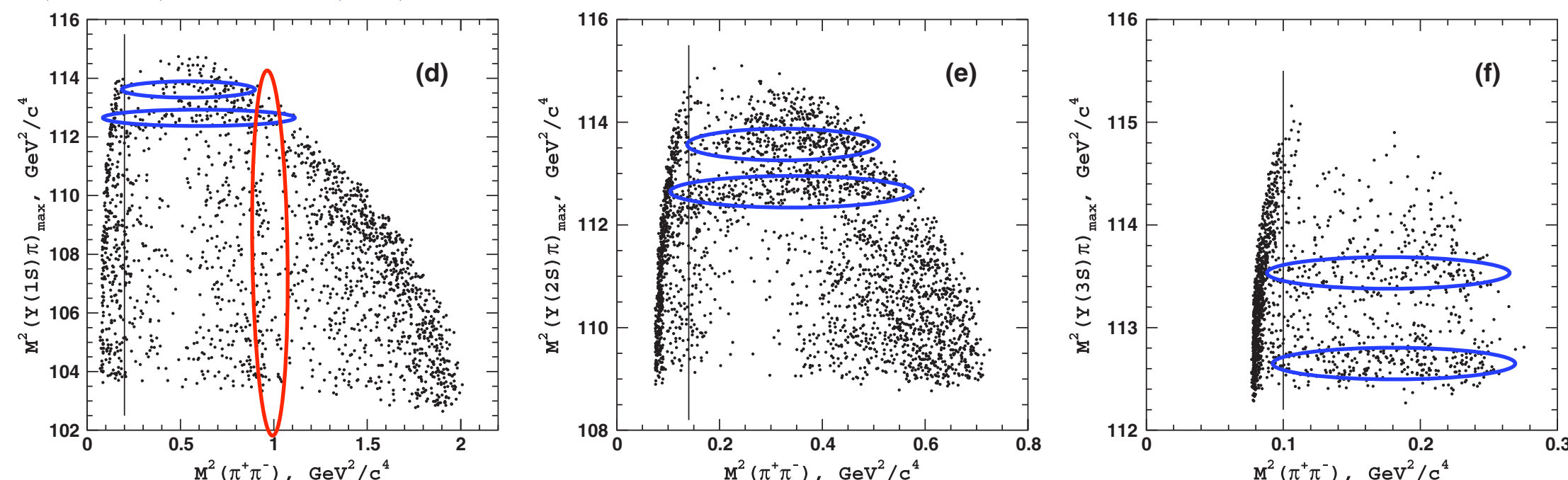
$$\Upsilon(10860) \rightarrow \pi B^{(*)} \bar{B}^*$$

- Invariant mass distributions in BB^* , B^*B^* and $h_b(mP)\pi$ channels



- Dalitz plot for $\Upsilon(10860) \rightarrow \pi\pi\Upsilon(nS)$ and its projections to $\Upsilon(nS)\pi$ and $\pi\pi$

contains
 Z_b 's in $\Upsilon(nS)\pi$
but also $\pi\pi$ FSI,
e.g. from $f_0(980)$



$Z_b(10610)$ and $Z_b(10650)$. Known Facts

- Location: very near S-wave thresholds of two hadrons $B\bar{B}^*$, $B^*\bar{B}^*$
- Dominant decays to these open-flavour channels
- $Z_b^{(')}$ are clearly exotics: seen in charged modes $\pi^\pm h_b(mP)$, $\pi^\pm \Upsilon(nS)$
 \Rightarrow must be made of ≥ 4 quarks
- $\text{Br}[\Upsilon(10860) \rightarrow \pi\pi h_b(mP)] \simeq \text{Br}[\Upsilon(10860) \rightarrow \pi\pi \Upsilon(nS)]$
 - Heavy quark spin flip
 - No spin flipTalk by Alexander Bondar
on Monday

Natural explanation :

- (a) the decays go through Z_b 's and
- (b) Z_b 's are molecules

$$|Z_b\rangle = -\frac{1}{\sqrt{2}} \left[(1_{b\bar{b}}^- \otimes 0_{q\bar{q}}^-)_{S=1} + (0_{b\bar{b}}^- \otimes 1_{q\bar{q}}^-)_{S=1} \right]$$

$$|Z'_b\rangle = +\frac{1}{\sqrt{2}} \left[(1_{b\bar{b}}^- \otimes 0_{q\bar{q}}^-)_{S=1} - (0_{b\bar{b}}^- \otimes 1_{q\bar{q}}^-)_{S=1} \right]$$

Bondar, Garmash, Milstein, Mizuk, and Voloshin
PRD 84, 054010 (2011)

$\Rightarrow Z_b(10610)/Z_b(10650)$ are strong candidates for hadronic molecules

This Talk is about

- $Z_b(10610)$ and $Z_b(10650)$ from decays:

$$\Upsilon(10860) \rightarrow \pi Z_b^{(\prime)} \rightarrow \pi B^{(*)} \bar{B}^*$$

$$\Upsilon(10860) \rightarrow \pi Z_b^{(\prime)} \rightarrow \pi\pi h_b(mP)$$

Wang, VB, Filin, Hanhart, Nefediev, and Wijnen PRD 98, 074023 (2018)

- Simultaneous analysis of these line shapes in chiral EFT approach with coupled-channels
- Fixing LECs and extracting Z_b poles and residues
- Predictions for HQSS partners is not discussed here, see

VB, Epelbaum, Filin, Hanhart, Nefediev, and Wang PRD 99, 094013 (2019)

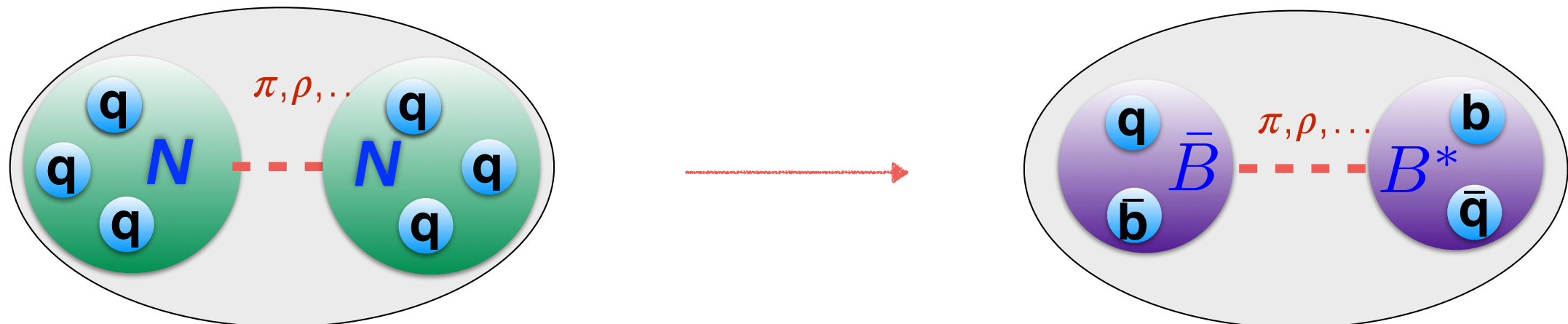
- Insights into the nature of the $Z_b(10610)$ and $Z_b(10650)$ from $\Upsilon(10860) \rightarrow \Upsilon(nS) \pi^+ \pi^-$ ($n=1,2,3$)

VB, Epelbaum, Filin, Hanhart, Mizuk, Nefediev and Roperz PRD 103, 034016 (2021)

- Multichannel Dalitz plot analysis using the same EFT approach from above as input
- Focus is put on $\pi\pi/KK$ final-state interactions (FSI) and the consistency check

EFT for heavy-hadron molecules

our work PRD 98, 074023 (2018)



Underlying idea: Forces are similar to NN potential

Voloshin, Okun (1976)

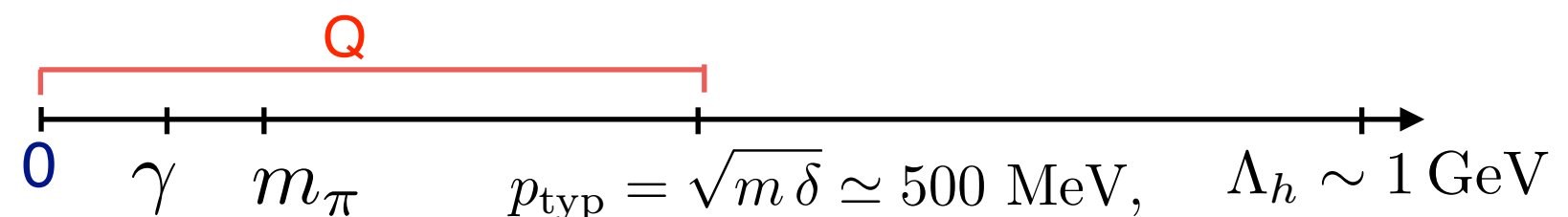
New insights: coupled-channel effects and consequences from HQSS

Goals: Analyse exp. line shapes including the energy range between $B\bar{B}^*$ and $B^*\bar{B}^*$

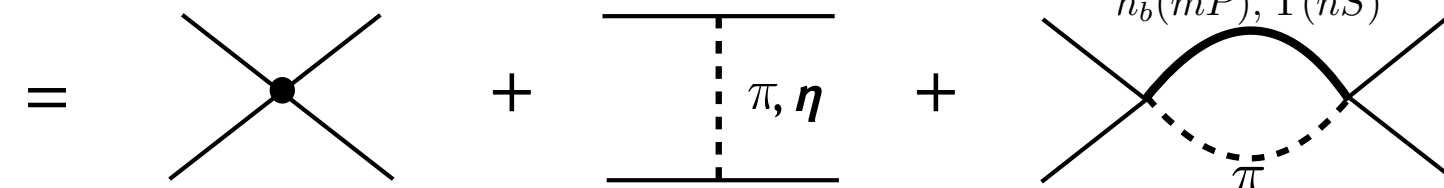
Tools: Coupled-channel potentials respecting HQSS and chiral symmetry

Elastic potential to a given order in Q/Λ_h :

👉 typical soft scale Q



$V_{\text{LO}}^{\text{eff}}$



Formalism for line shapes $\Upsilon(10860) \rightarrow \pi Z_b^{(')} \rightarrow \pi\alpha$

- Production amplitudes for the events dominated by the Zb's poles:

$$U_{\text{el}} = \begin{array}{c} \text{---} \\ \text{---} \\ \text{---} \end{array} \pi + \begin{array}{c} \text{---} \\ \text{---} \\ \text{---} \end{array} \pi + \begin{array}{c} \text{---} \\ \text{---} \\ \text{---} \end{array} \pi$$

$$U_{\text{inel}} = \begin{array}{c} \text{---} \\ \text{---} \\ \text{---} \end{array} \pi + \begin{array}{c} \text{---} \\ \text{---} \\ \text{---} \end{array} \pi$$

$\Upsilon(5S)$ $B^{(*)}$ \bar{B}^* B \bar{B}^* $B^{(*)}$ \bar{B}^* \bar{B}^* $B^{(*)}$
 \bar{B}^* B \bar{B}^* \bar{B}^* \bar{B}^* \bar{B}^* \bar{B}^* \bar{B}^* $B^{(*)}$
 \bar{B}^* B \bar{B}^* π π \bar{B}^* \bar{B}^* \bar{B}^* π
 π $h_b(mP)$ $h_b(mP)$

$$T_{\alpha\beta} = V_{\alpha\beta}^{\text{eff}} - \sum_{\gamma} \int \frac{d^3 q}{(2\pi)^3} V_{\alpha\gamma}^{\text{eff}} G_{\gamma} T_{\gamma\beta}$$

- Input: experimental distributions for

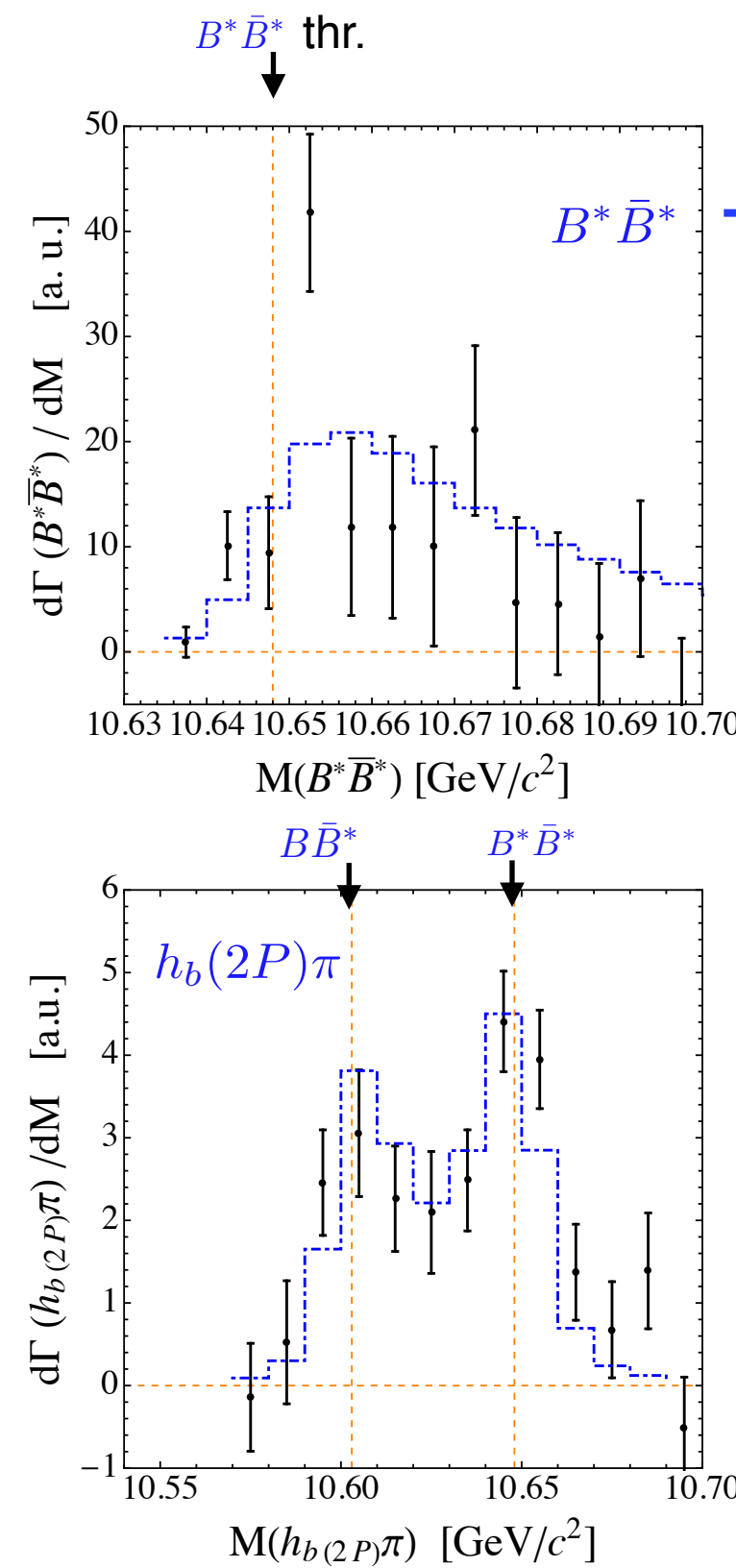
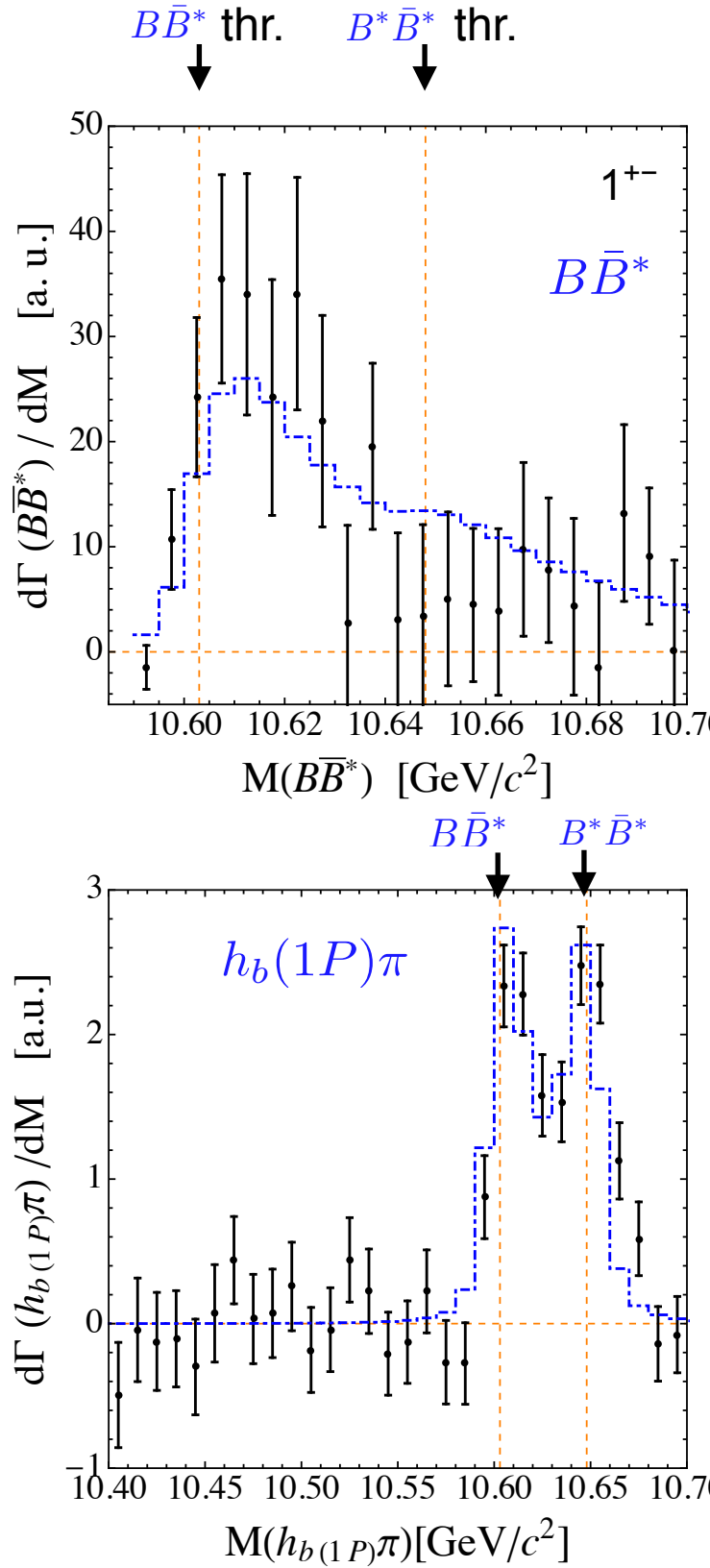
$$\Upsilon(10860) \rightarrow \pi Z_b^{(')} \rightarrow \pi\alpha \quad \alpha = BB^*, \quad B^*B^*, \quad h_b(1P)\pi, \quad h_b(2P)\pi$$

and branching fractions for $\alpha = B\bar{B}^*, \quad B^*\bar{B}^*, \quad h_b(1P)\pi, \quad h_b(2P)\pi, \quad \Upsilon(1S)\pi, \quad \Upsilon(2S)\pi, \quad \Upsilon(3S)\pi$

Belle: Bondar et al. (2012), Garmash et al. (2016)

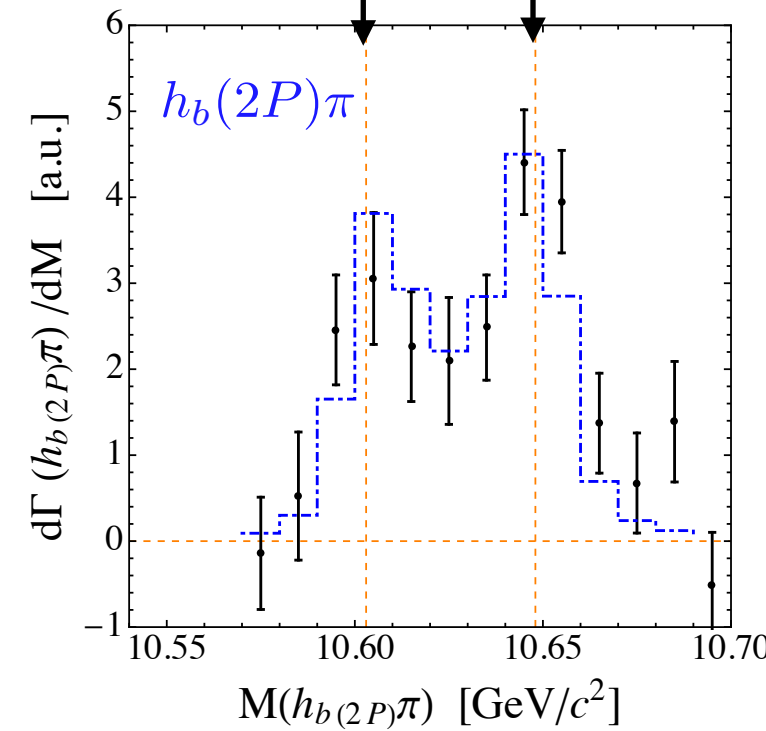
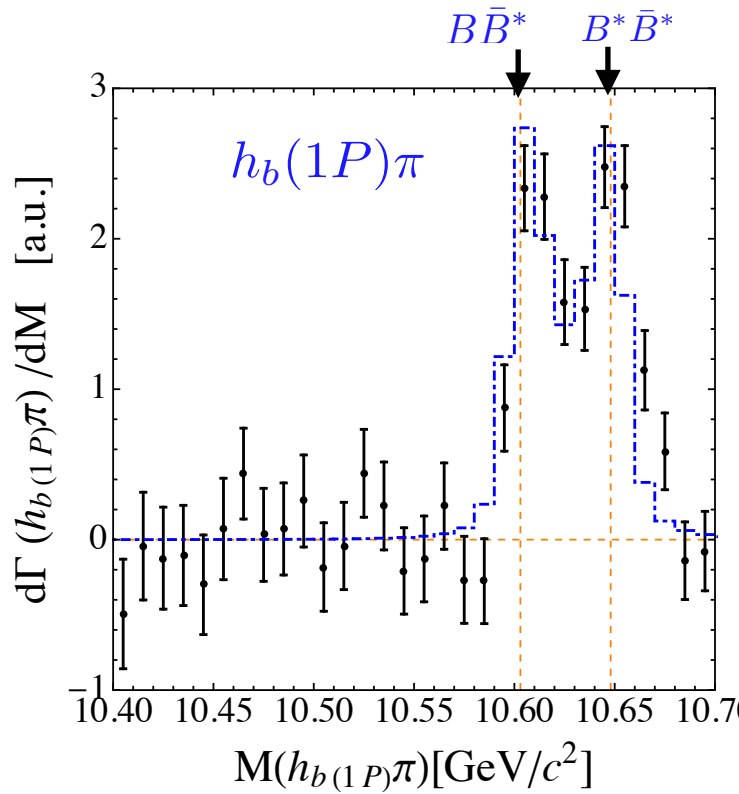
Results: pionless theory at LO

our work:
PRD 98, 074023 (2018)

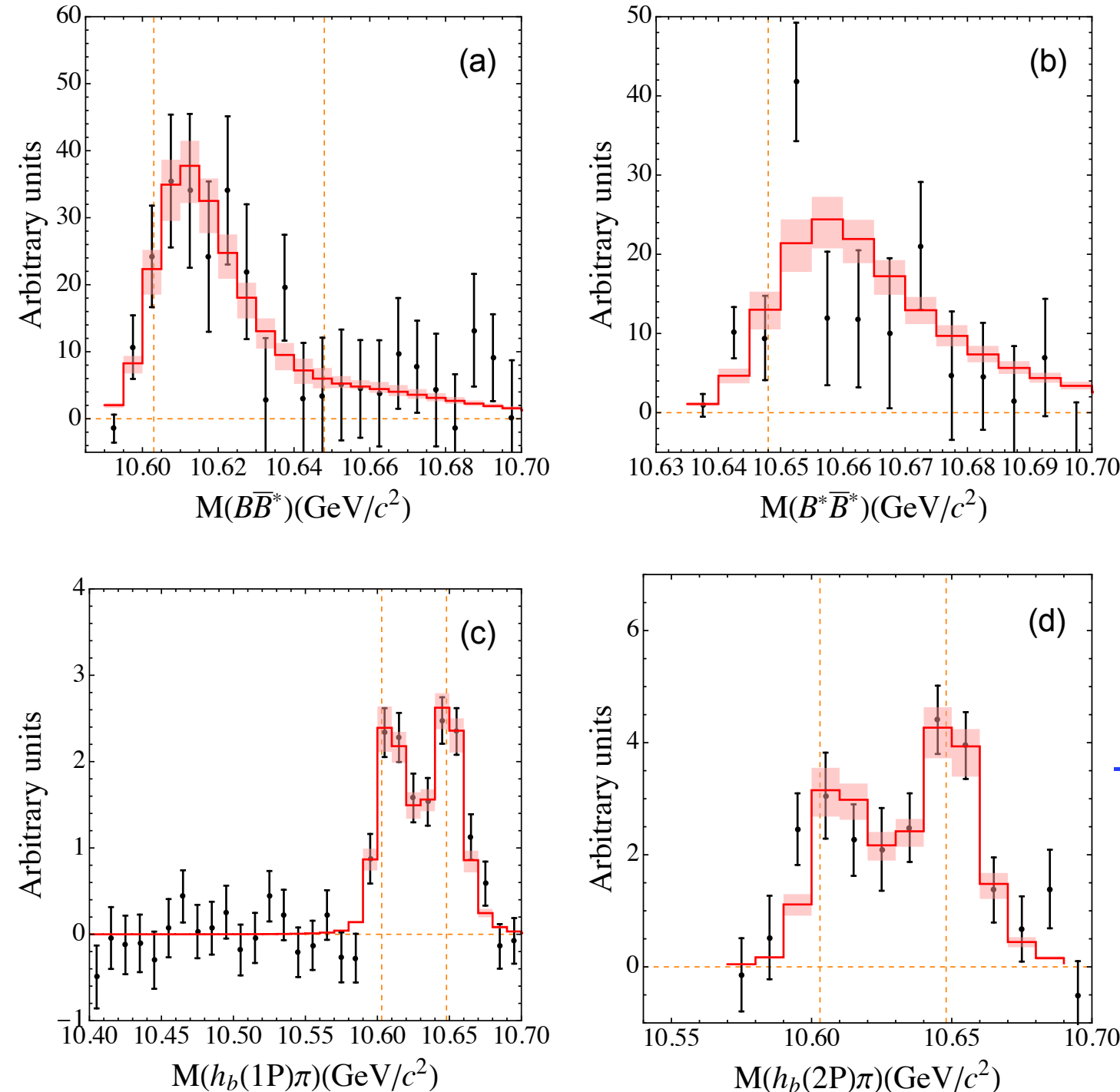


- HQSS is preserved in the potentials

- Z_b 's are virtual states



Final remarks from $\Upsilon(10860) \rightarrow \pi Z_b^{(\prime)} \rightarrow \pi\pi h_b(mP)$



- Visible effect from tensor part of OPE
- $\chi^2=1.29$ → $\chi^2=0.95$
- Zb's: virtual states → resonances
- All LECs are extracted from the best fit including 1σ errors
- Natural suppression of higher-order terms
- Data are consistent with HQSS respecting interactions

J^{PC}	State	Threshold	E_B w.r.t. threshold, [MeV]	Residue at pole
1^{+-}	Z_b	$B\bar{B}^*$	$(-2.3 \pm 0.5) - i(1.1 \pm 0.1)$	$(-1.2 \pm 0.2) + i(0.3 \pm 0.2)$
1^{+-}	Z'_b	$B^*\bar{B}^*$	$(1.8 \pm 2.0) - i(13.6 \pm 3.1)$	$(1.5 \pm 0.2) - i(0.6 \pm 0.3)$

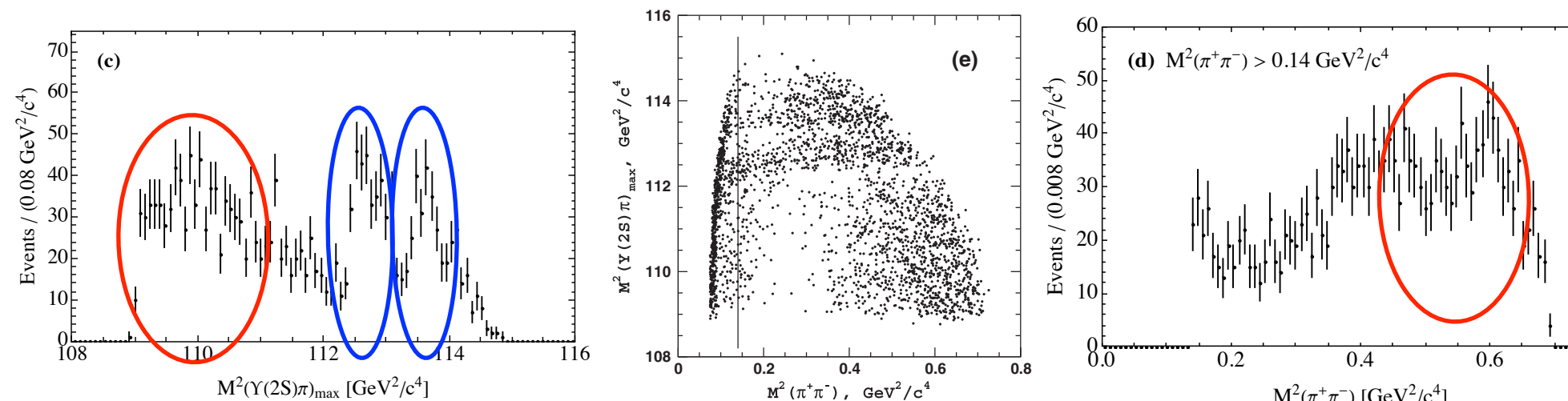
$\Upsilon(10860) \rightarrow \Upsilon(nS) \pi^+ \pi^-$: Goals and Tools

our work:
PRD 103, 034016 (2021)

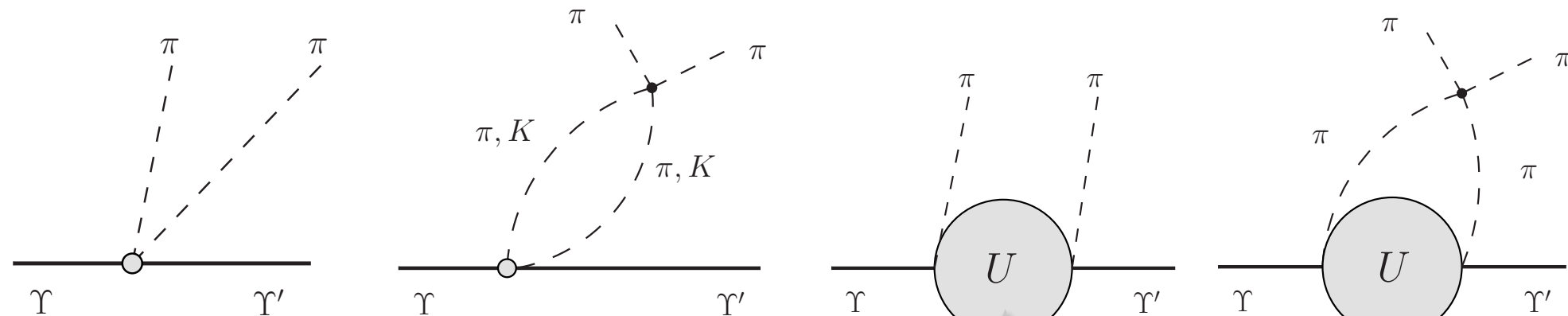
- High-statistic data by Belle

- Both $\pi\pi$ and $\pi\Upsilon$ play a role simultaneously!

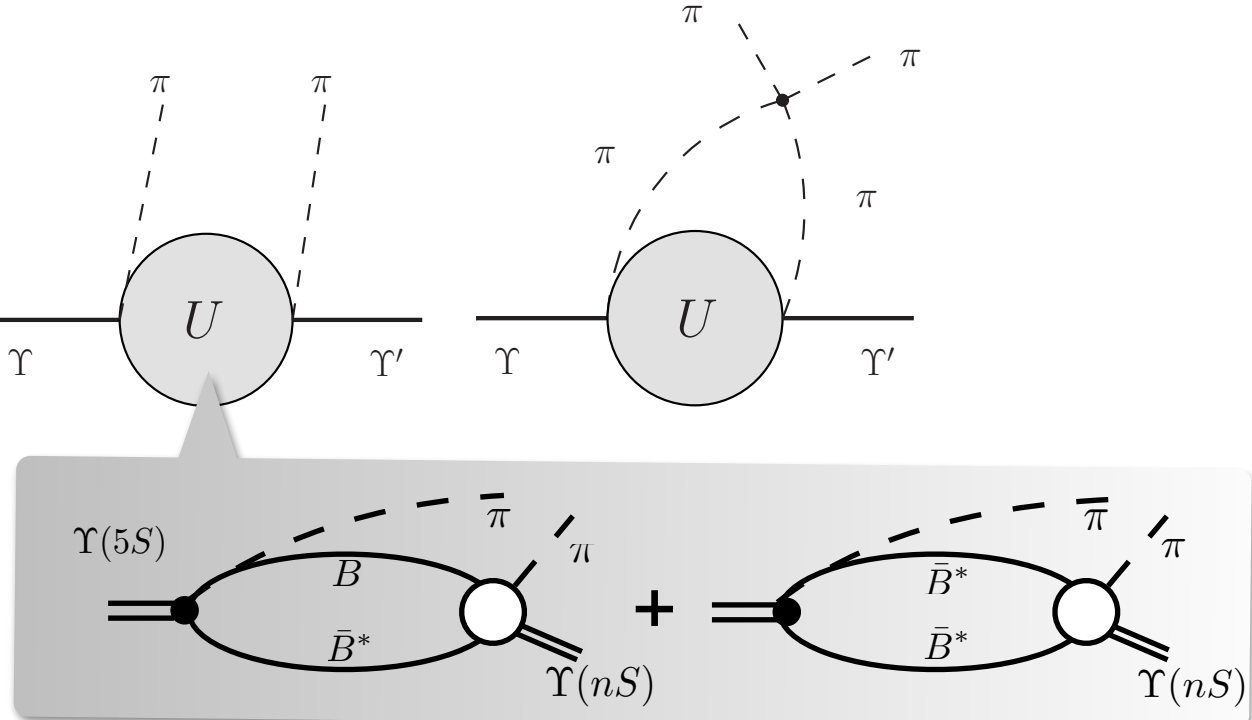
→ Analyse Dalitz plot



- Production: contact and coupled-channel via B-meson loops, as formulated above



U is a *parameter-free input* from a simple but realistic pionless scheme



- Dispersive approach to account for the $\pi\pi$ -KK FSI
- Important consistency check with previous results!

Dispersion relations for $\pi\pi$ - $K\bar{K}$ FSI

S-wave projection: $M_0(s) = \frac{1}{2} \int_{-1}^{+1} dz M(s, t, u) \equiv M_0^L + M_0^R$

Left-hand cut piece Right-hand cut piece with FSI

Dispersive reconstruction
of $\hat{M}_0^R(s)$ via $\hat{M}_0^L(s)$

$$\hat{M}_0(s) = \hat{M}_0^L(s) + \frac{\hat{\Omega}_0(s)}{\pi} \int_{4m_\pi^2}^\infty ds' \frac{\hat{\Omega}_0^{-1}(s') \hat{T}(s') \hat{\sigma}(s') \hat{M}_0^L(s')}{s' - s - i0}$$

$\pi\pi$ - $K\bar{K}$ scattering amplitude: $\hat{T}(s) = \begin{pmatrix} T_{\pi\pi \rightarrow \pi\pi} & T_{\pi\pi \rightarrow K\bar{K}} \\ T_{K\bar{K} \rightarrow \pi\pi} & T_{K\bar{K} \rightarrow K\bar{K}} \end{pmatrix} = \begin{pmatrix} \frac{\eta e^{2i\delta} - 1}{2i\sigma_\pi} & ge^{i\psi} \\ ge^{i\psi} & \frac{\eta e^{2i(\psi-\delta)} - 1}{2i\sigma_K} \end{pmatrix}$

R. Garcia-Martin et al., PRD83, 074004 (2011), I. Caprini et al., EPJC72, 1860 (2012), P. Buettiker et al., EPJC33, 409 (2004), L.Y.Dai et al., PRD90, 036004 (2014).

multichannel Omnès function: $\hat{\Omega}_0(s) = \frac{1}{\pi} \int_{4m_\pi^2}^\infty ds' \frac{\hat{T}^*(s') \hat{\sigma}(s) \hat{\Omega}_0(s')}{s' - s - i0}$

$$\eta = \sqrt{1 - 4g^2 \sigma_\pi \sigma_K \theta(s - 4m_K^2)}$$

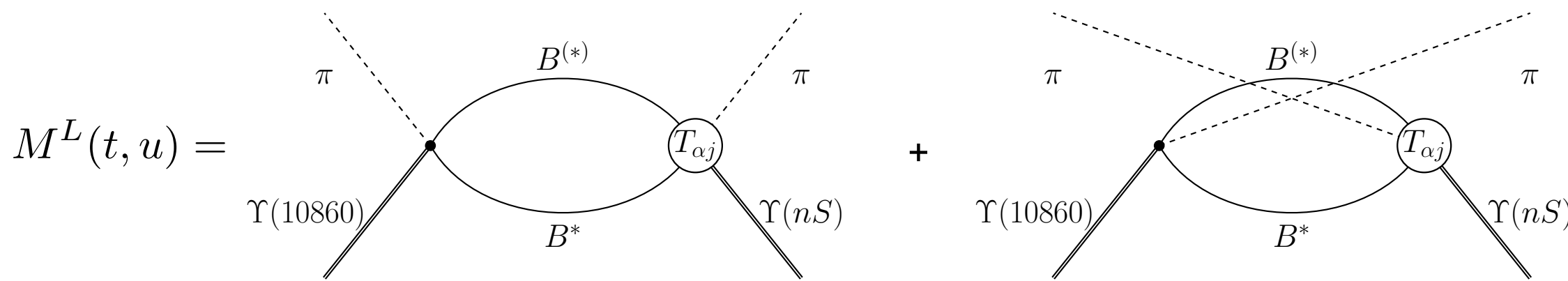
$$\hat{\sigma}(s) = \text{diag}\{\sigma_\pi, \sigma_K\}$$

$$\sigma_P(s) = \sqrt{1 - s_P^{\text{th}}/s}$$

$$P = \pi, K$$

Production via $\pi\pi$ mode: $\hat{M}_0^L = ([M_0^L]_{\pi\pi}, 0)^T$

Left-hand cut production amplitude



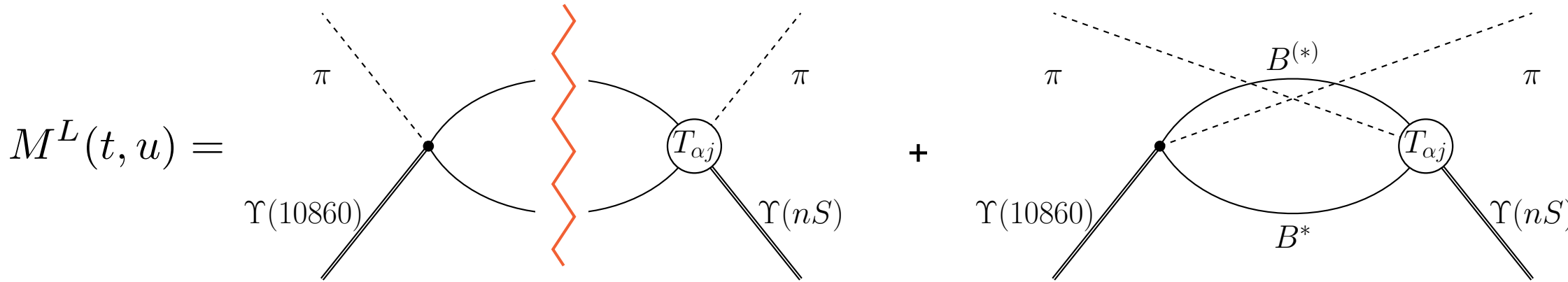
$$M^L(t, u) = U(t) + U(u) = -\frac{1}{\pi} \int_{(m_\pi + m_{\Upsilon(1S)})^2}^{\infty} d\mu^2 \operatorname{Im} U(\mu^2) \left(\frac{1}{t - \mu^2} + \frac{1}{u - \mu^2} \right)$$

→ **S-wave**
→ **projection**

$$M_0^L(s)$$

- $Z_b(10610)/Z_b(10650)$ are poles in the coupled-channel amplitudes $M^L(t, u)$

Left-hand cut production amplitude



$$M^L(t, u) = U(t) + U(u) = -\frac{1}{\pi} \int_{(m_\pi + m_{\Upsilon(1S)})^2}^{\infty} d\mu^2 \operatorname{Im} U(\mu^2) \left(\frac{1}{t - \mu^2} + \frac{1}{u - \mu^2} \right)$$

→ S-wave
→ projection $M_0^L(s)$

- $Z_b(10610)/Z_b(10650)$ are poles in the coupled-channel amplitudes $M^L(t, u)$
- $\operatorname{Im} M_0^L(s)$: Leading contribution is from the $B^{(*)}\bar{B}^*$ cuts, these states can be on shell
subleading one— from inelastic channels

Subtractions and matching to chiral contact amplitudes

$$\hat{M}_0(s) = \hat{M}_0^L(s) + \frac{\hat{\Omega}_0(s)}{\pi} \int_{4m_\pi^2}^\infty ds' \frac{\hat{\Omega}_0^{-1}(s') \hat{T}(s') \hat{\sigma}(s') \hat{M}_0^L(s')}{s' - s - i0}$$

- Dispersive Integral is convergent but details of $\pi\pi$ at large s are known badly
 \implies 2 subtractions with real coefficients
- $\text{Im } M_0^L(s)$ is under control, since it is driven by the $B^{(*)}\bar{B}^*$ cuts from the finite region of s
- In contrast, 2 complex coefficients were used in a related study of $e^+e^- \rightarrow \pi^+\pi^-\psi(2S)$

Molnar et al., PLB797, 134851 (2019)

Subtractions and matching to chiral contact amplitudes

$$\hat{M}_0(s) = \hat{M}_0^L(s) + \frac{\hat{\Omega}_0(s)}{\pi} \int_{4m_\pi^2}^\infty ds' \frac{\hat{\Omega}_0^{-1}(s') \hat{T}(s') \hat{\sigma}(s') \hat{M}_0^L(s')}{s' - s - i0}$$

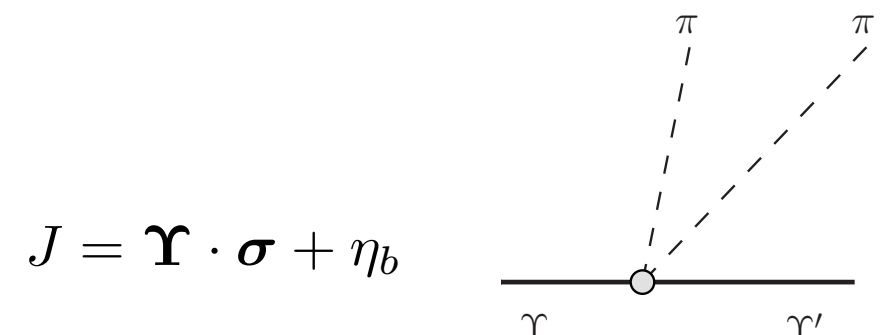
- Dispersive Integral is convergent but details of $\pi\pi$ at large s are known badly
 - \Rightarrow 2 subtractions with real coefficients

- $\text{Im } M_0^L(s)$ is under control, since it is driven by the $B^{(*)}\bar{B}^*$ cuts from the finite region of s
- In contrast, 2 complex coefficients were used in a related study of $e^+e^- \rightarrow \pi^+\pi^-\psi(2S)$

Molnar et al., PLB797, 134851 (2019)

- Matching to chiral expansion

$$\mathcal{L}_{\Upsilon\Upsilon'\Phi\Phi} = \frac{c_1}{2} \langle J^\dagger J' \rangle \langle u_\mu u^\mu \rangle + \frac{c_2}{2} \langle J^\dagger J' \rangle \langle u_\mu u_\nu \rangle v^\mu v^\nu + \text{h.c.}$$



$$u_\mu = i (u^\dagger \partial_\mu u - u \partial_\mu u^\dagger)$$

$$u = \exp \left(\frac{i\Phi}{\sqrt{2}f} \right)$$

$$\Phi = \begin{pmatrix} \frac{1}{\sqrt{2}}\pi^0 + \frac{1}{\sqrt{6}}\eta_8 & \pi^+ & K^+ \\ \pi^- & -\frac{1}{\sqrt{2}}\pi^0 + \frac{1}{\sqrt{6}}\eta_8 & K^0 \\ K^- & \bar{K}^0 & -\frac{2}{\sqrt{6}}\eta_8 \end{pmatrix}$$



$$\hat{M}_0^\chi(s) = \left(M_0^{\chi,\pi\pi}(s), \frac{2}{\sqrt{3}}M_0^{\chi,KK}(s) \right)^T$$

$$M_0^{\chi,PP}(s) = -\frac{2}{f_P^2} \sqrt{m_\Upsilon m_{\Upsilon'}} \left\{ c_1 (s - 2m_P^2) + \frac{c_2}{2} \left[s + q^2 \left(1 - \frac{\sigma_P^2(s)}{3} \right) \right] \right\}$$

Chen et al. PRD93, 034030 (2016),
PRD95, 034022 (2017)

Final results for $M(s,t,u)$

$$M(s, t, u) = M^L(t, u) + \hat{\Omega}_0(s) \left(\hat{M}_0^{\chi, \pi\pi}(s) + \hat{I}_0^{(2)}(s) \right) + \Omega_2(s) M_2^{\chi, \pi\pi}(s) P_2(z)$$

coupled-channel production amplitude, contains all partial waves
chiral contact term
dispersive integral
D-wave contribution

$$\hat{I}_0^{(2)}(s) = \frac{s^2}{\pi} \int_{4m_\pi^2}^\infty \frac{ds'}{s'^2} \frac{\hat{\Omega}_0^{-1}(s') \hat{T}(s') \hat{\sigma}(s') \text{Re} M_0^L(s')}{s' - s - i0} + \frac{i}{\pi} \int_{4m_\pi^2}^\infty ds' \frac{\hat{\Omega}_0^{-1}(s') \hat{T}(s') \hat{\sigma}(s') \text{Im} M_0^L(s')}{s' - s - i0} + \hat{I}_0^{\text{anom}}(s)$$

twice-subtracted
unsubtracted
anomalous contribution

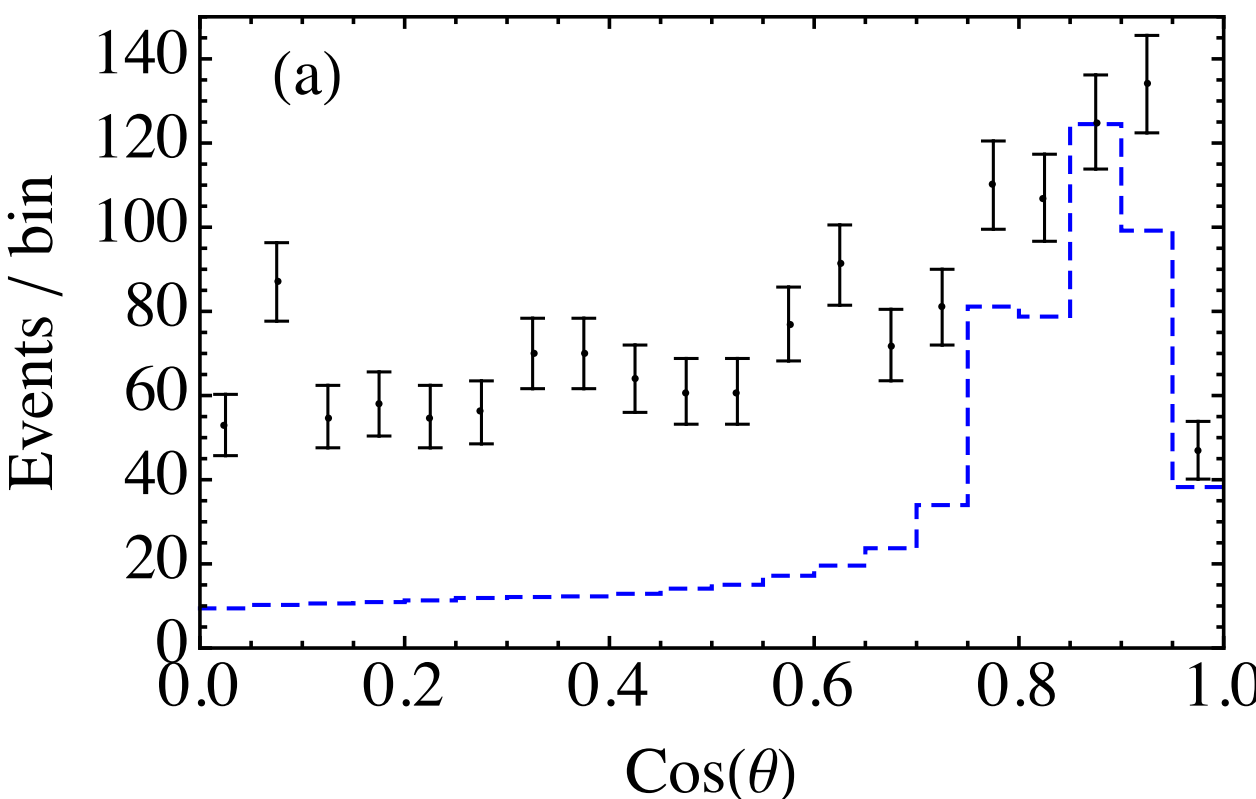
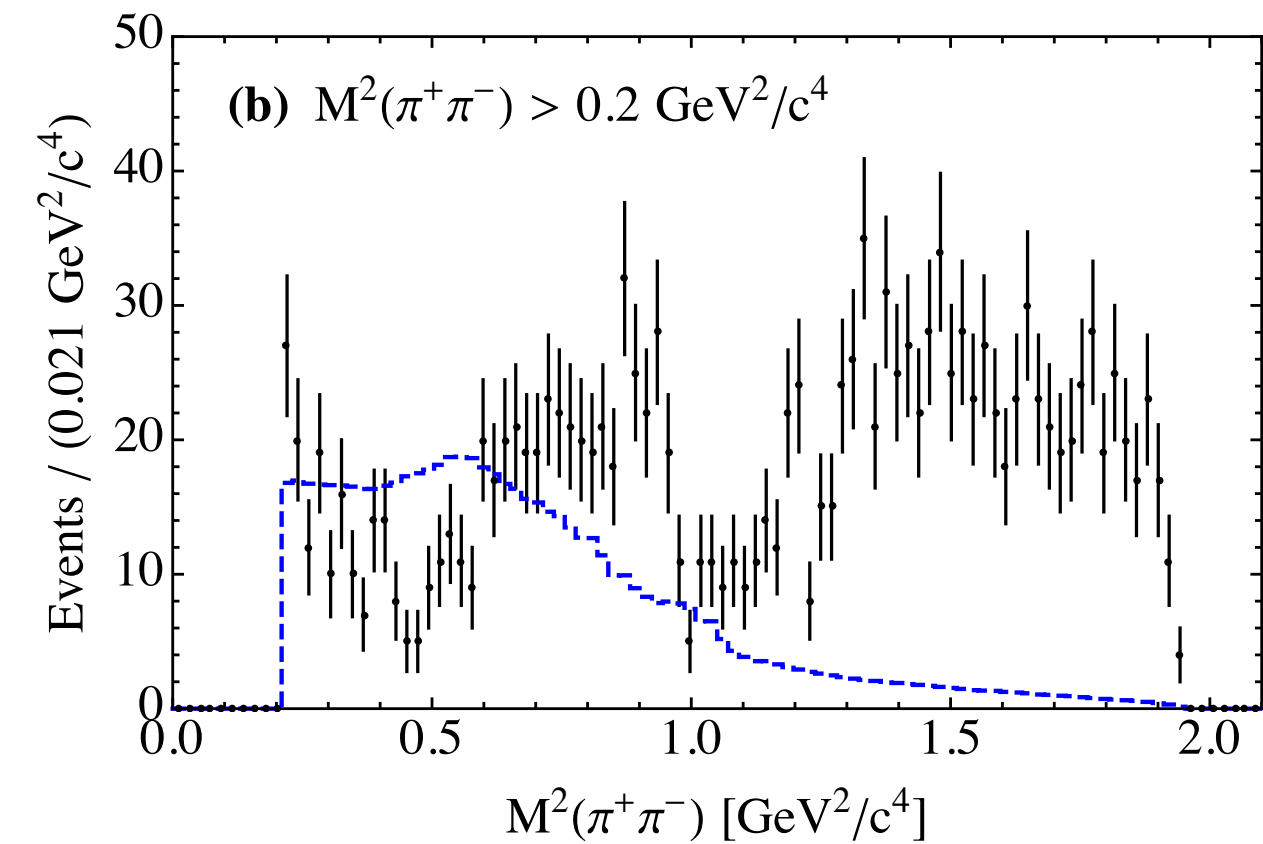
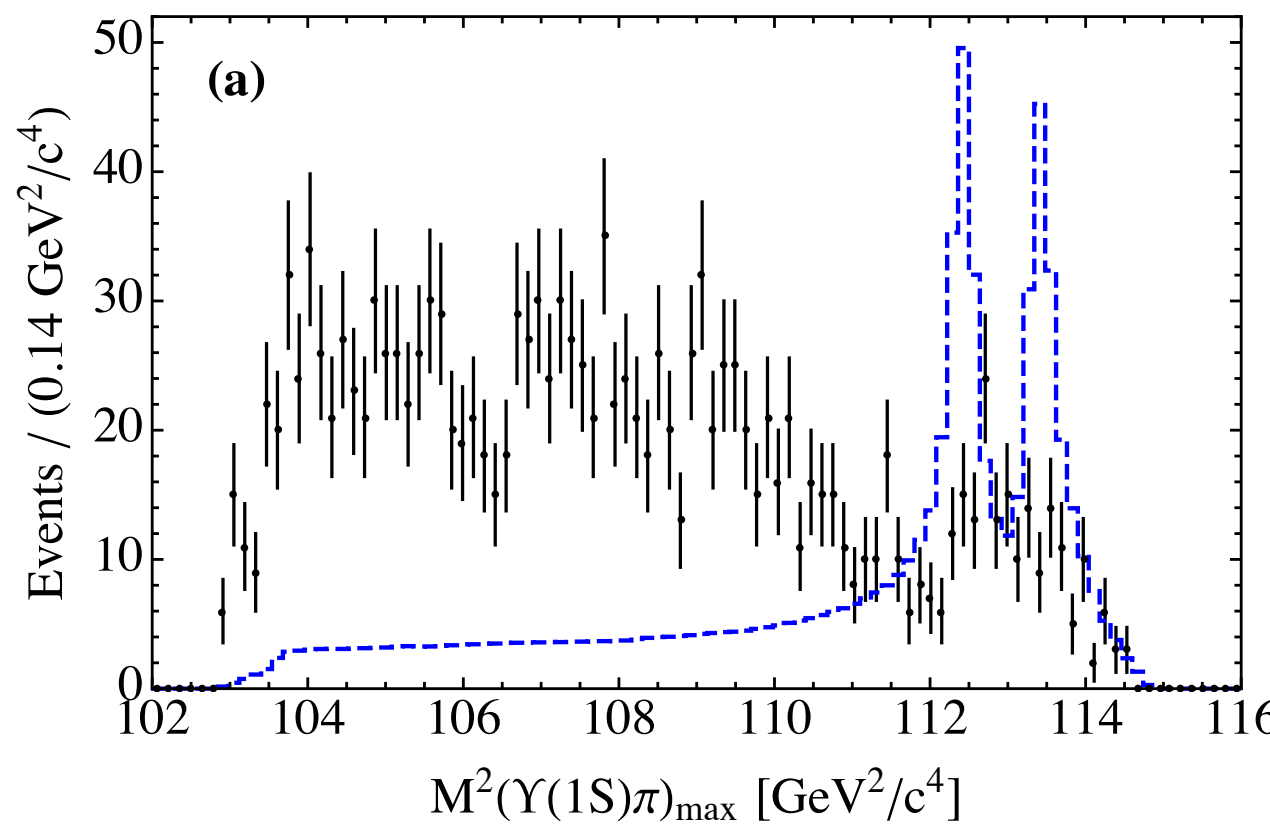
- All the parameters from a coupled-channel approach in $M^L(t,u)$ fixed from data to the decays

$$\Upsilon(10860) \rightarrow \pi Z_b^{(\prime)} \rightarrow \pi B^{(*)} \bar{B}^* \quad \text{and} \quad \Upsilon(10860) \rightarrow \pi Z_b^{(\prime)} \rightarrow \pi\pi h_b(mP)$$

- Parameters in the fits: overall normalization \mathcal{N} and chiral LECs $c1$ and $c2$

Dalitz plot projections: Individual Contrib's.

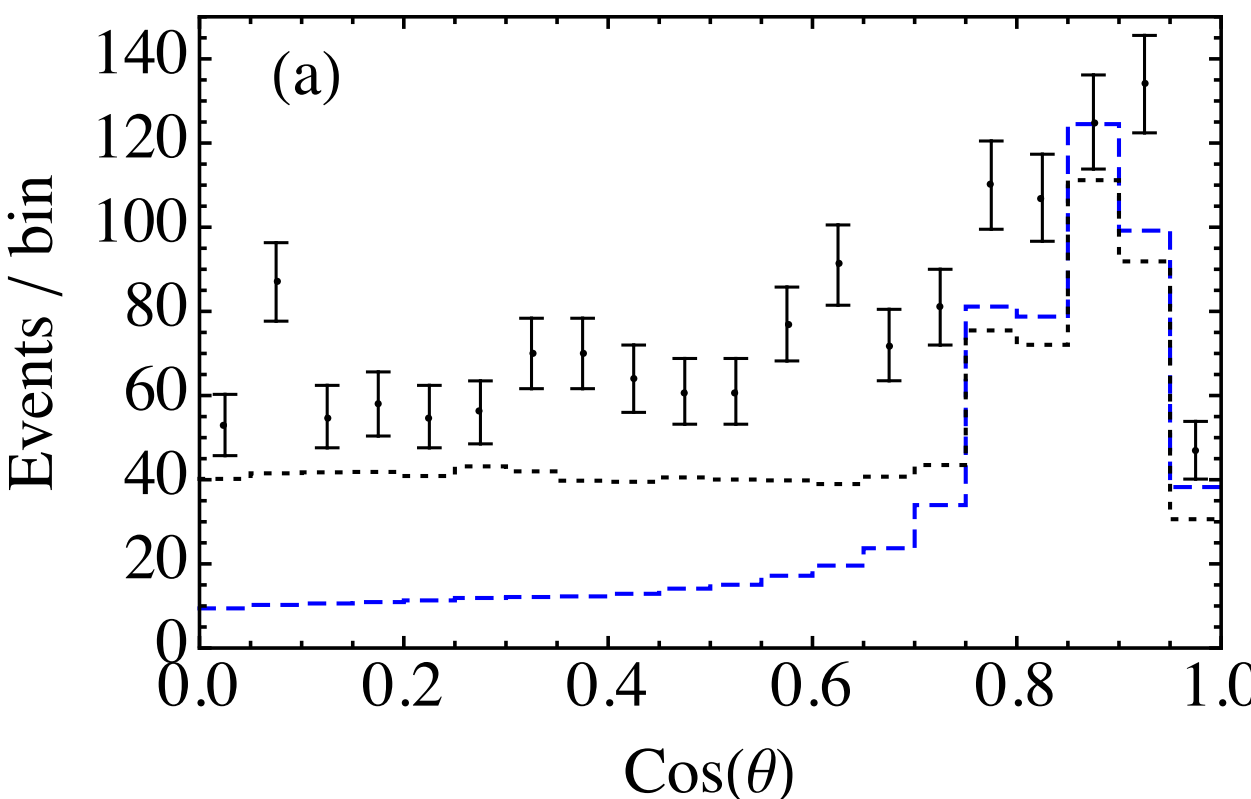
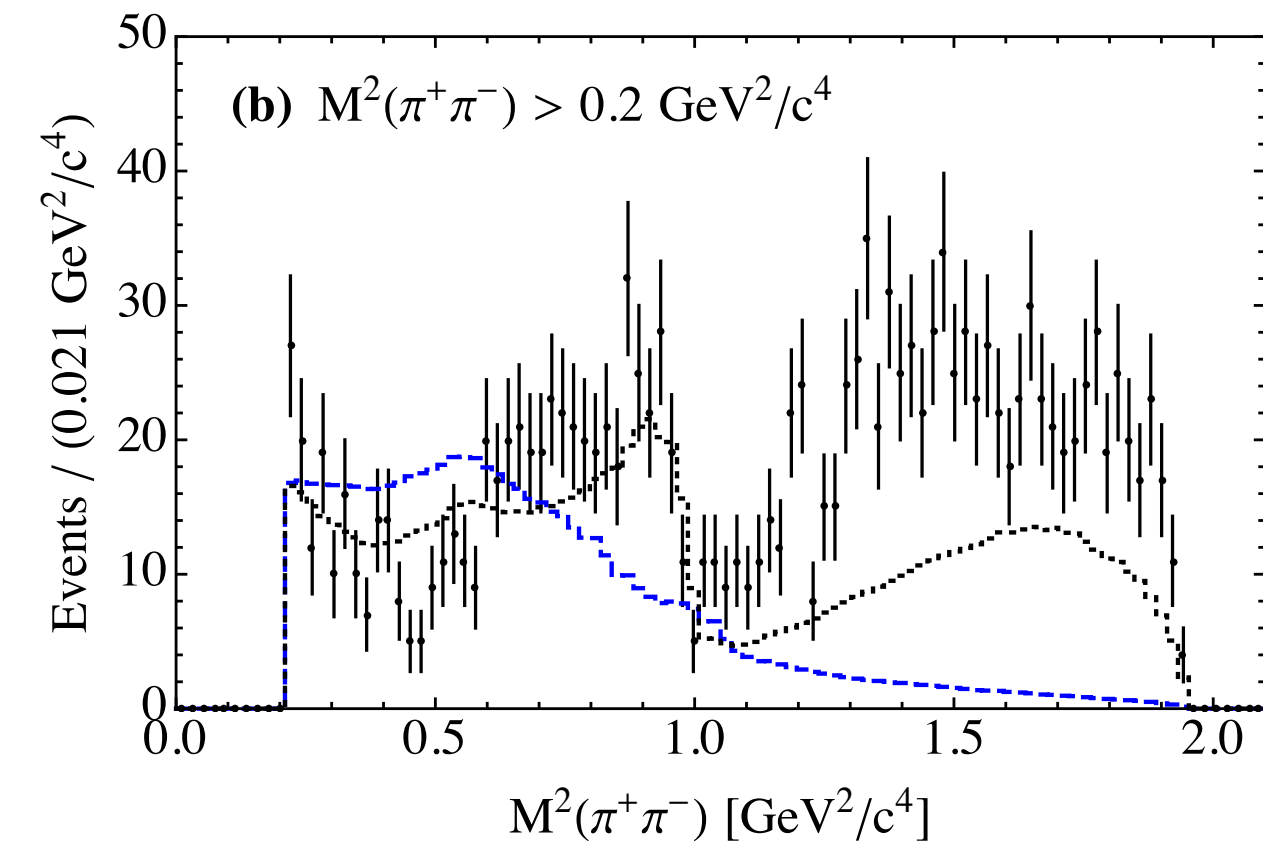
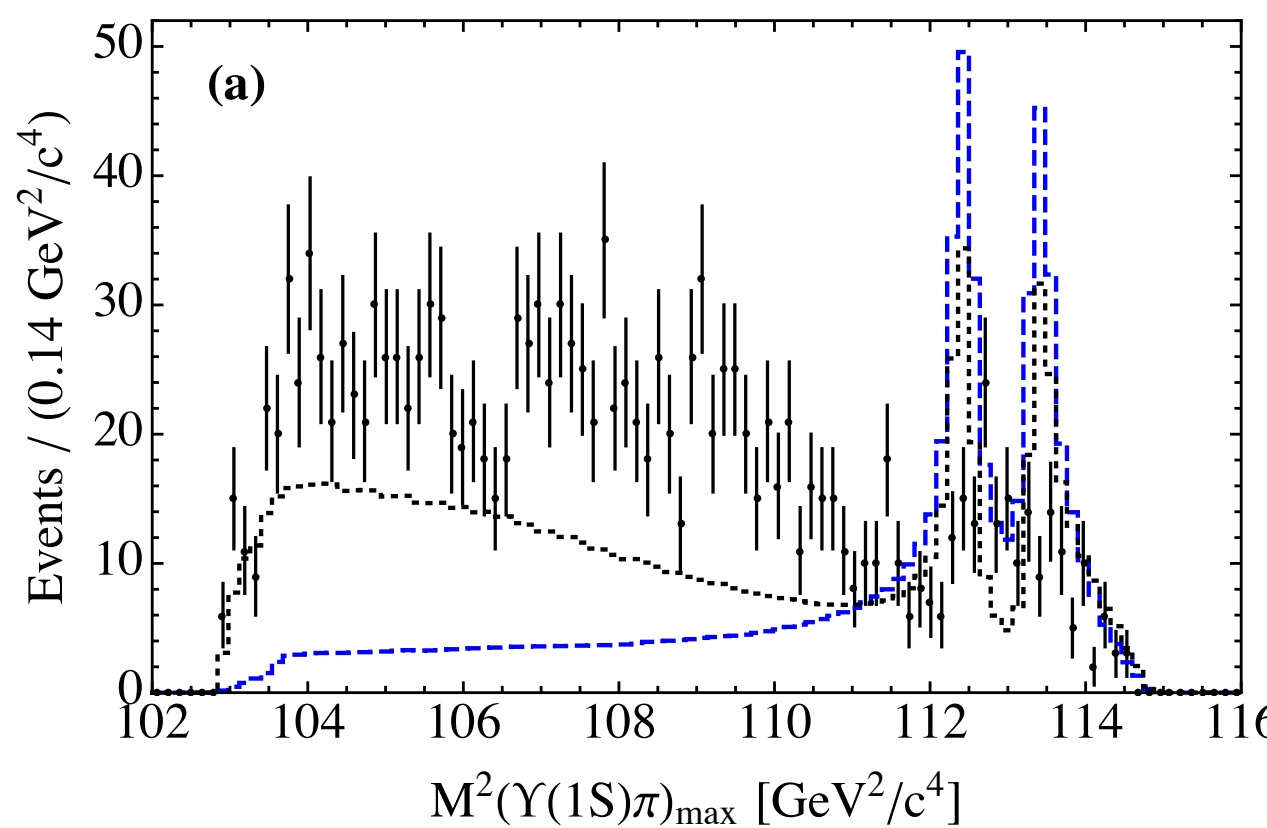
$\Upsilon(10860) \rightarrow \Upsilon(1S) \pi^+ \pi^-$



$$M^L(t, u) = U(t) + U(u) \quad \text{"Z}_b\text{"}$$

Dalitz plot projections: Individual Contrib's.

$\Upsilon(10860) \rightarrow \Upsilon(1S) \pi^+ \pi^-$

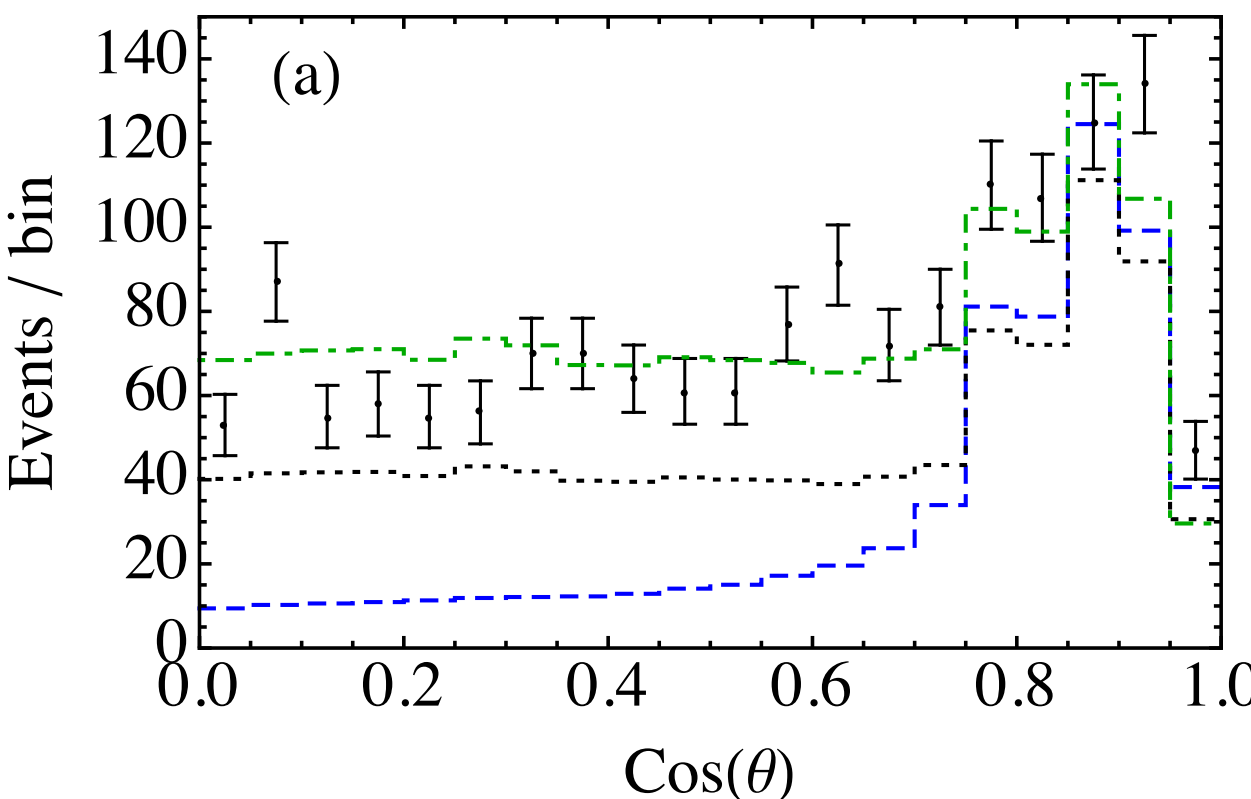
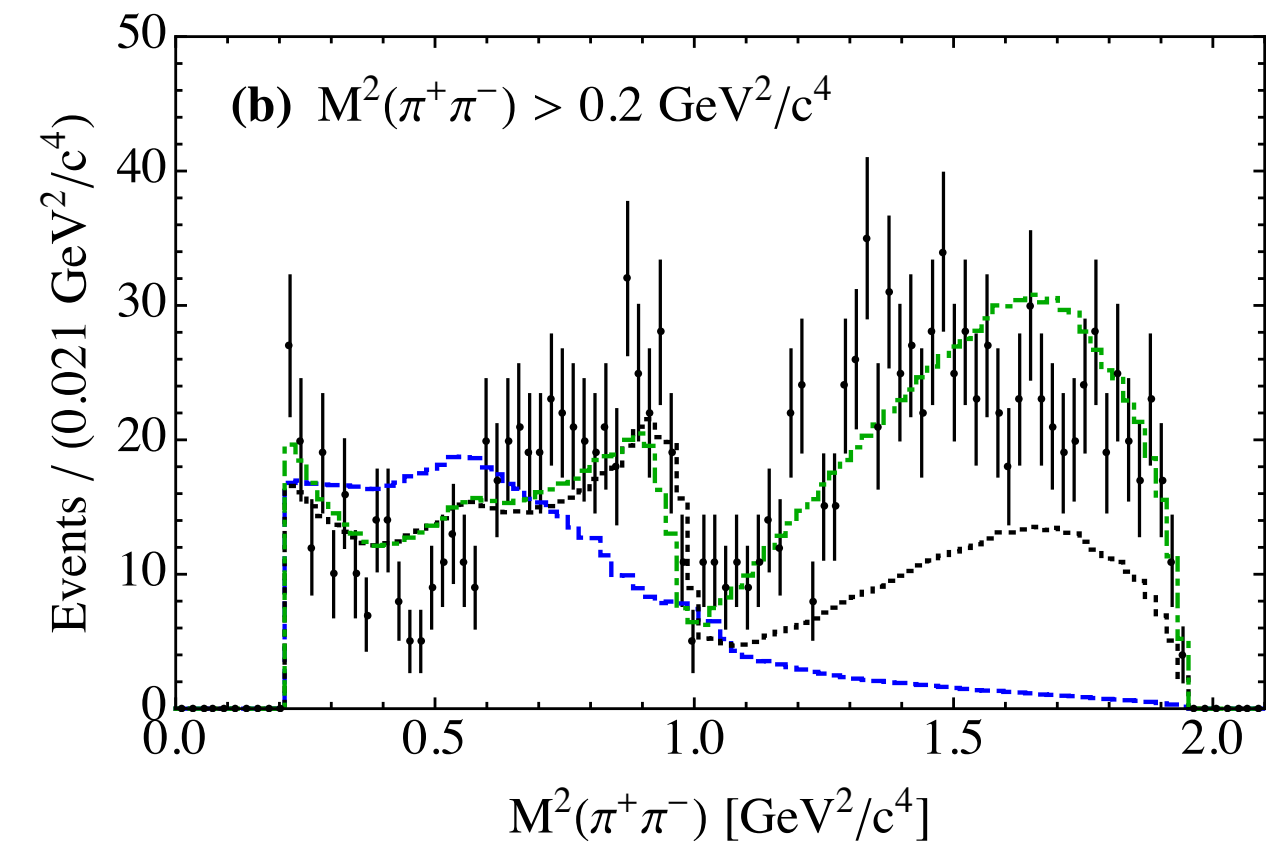
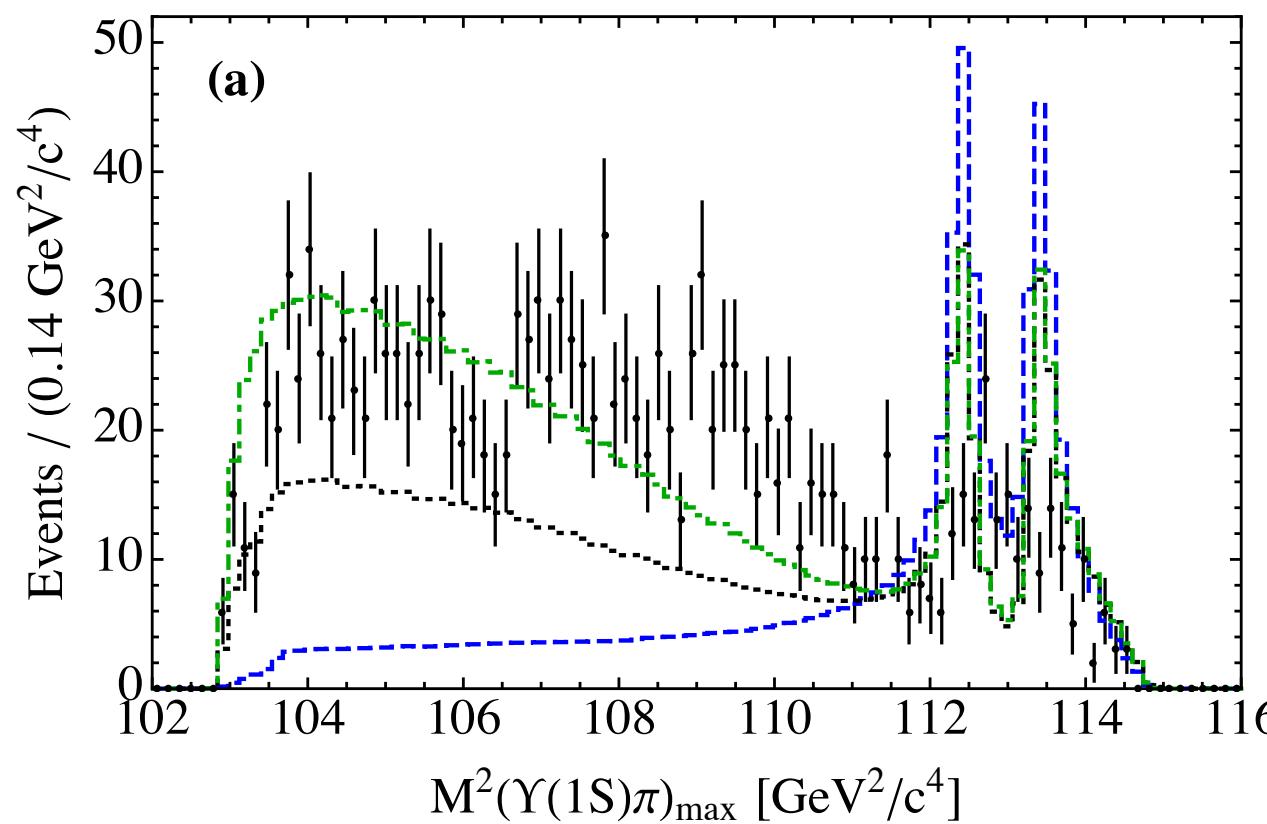


$$M^L(t, u) = U(t) + U(u) \quad \text{"Z}_b\text{"}$$

+ dispersive integral

Dalitz plot projections: Individual Contrib's.

$\Upsilon(10860) \rightarrow \Upsilon(1S) \pi^+ \pi^-$



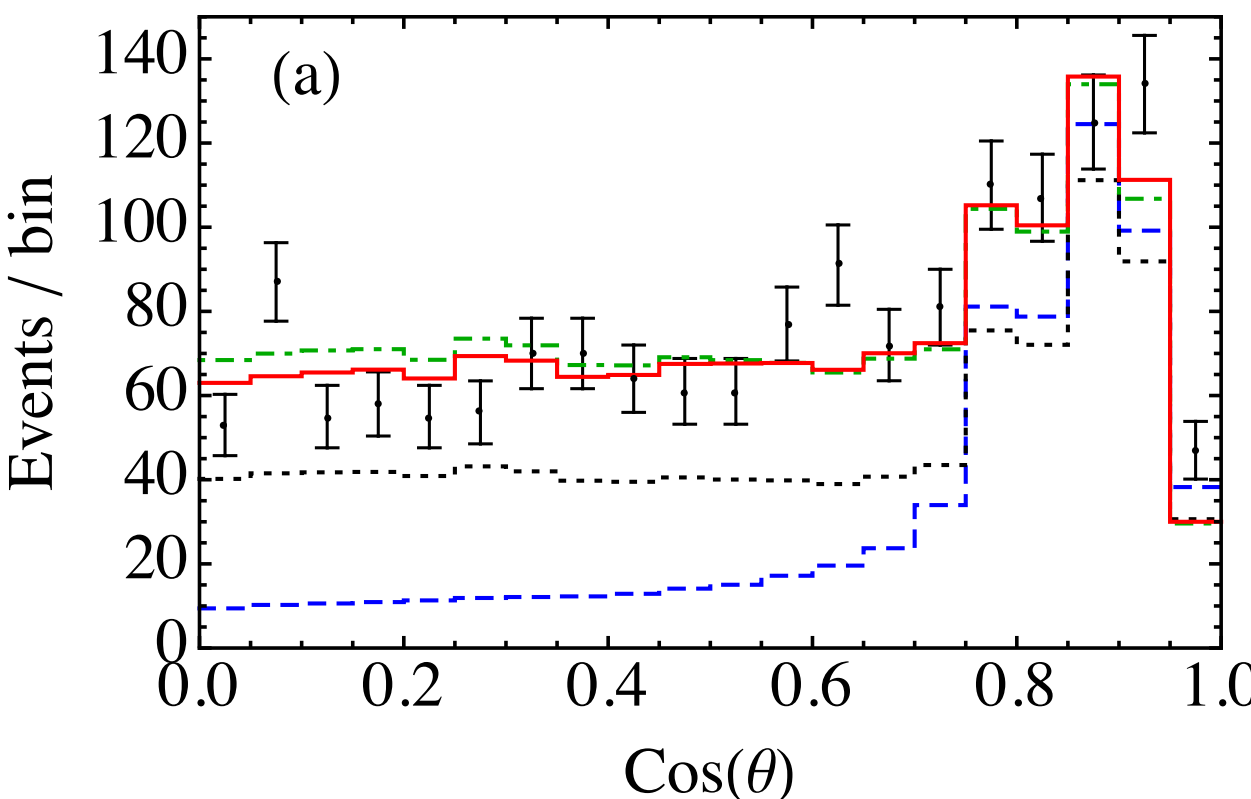
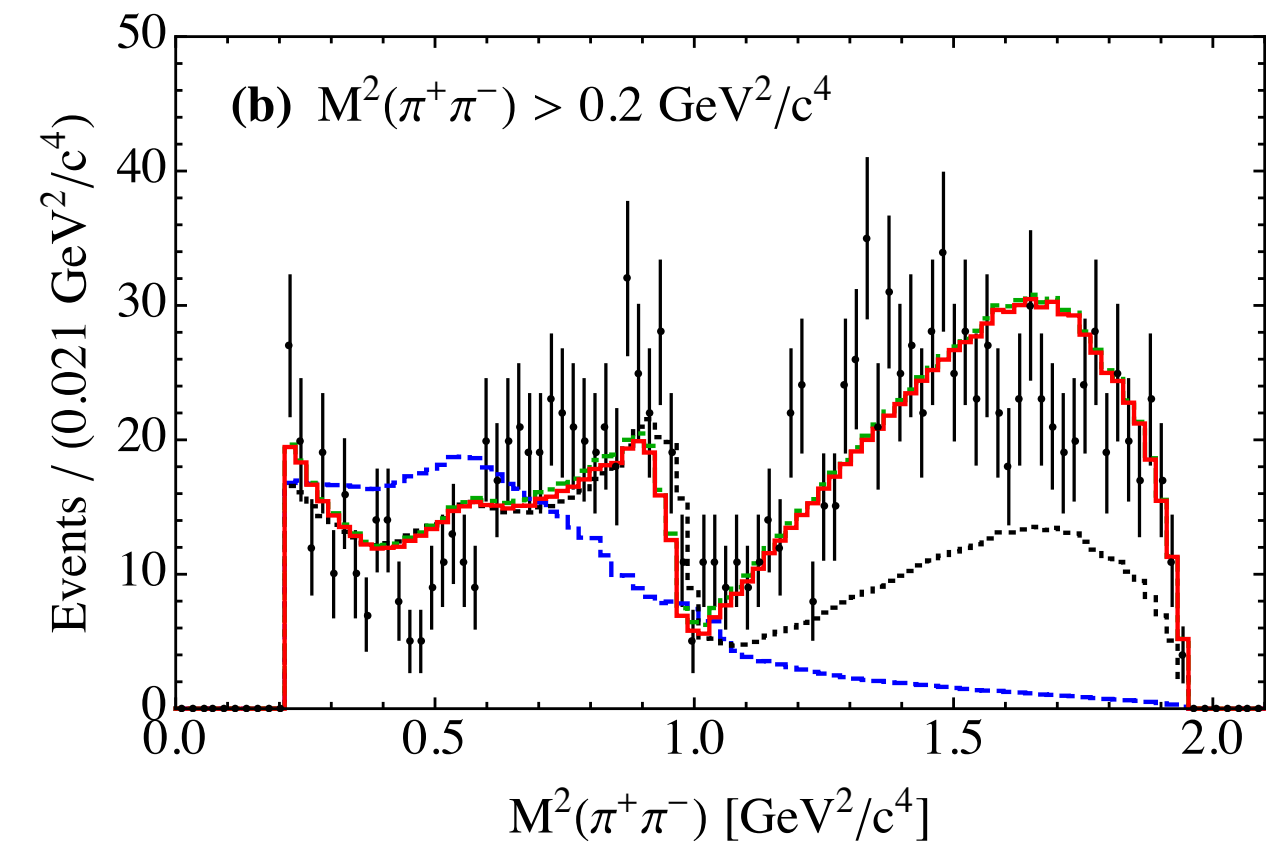
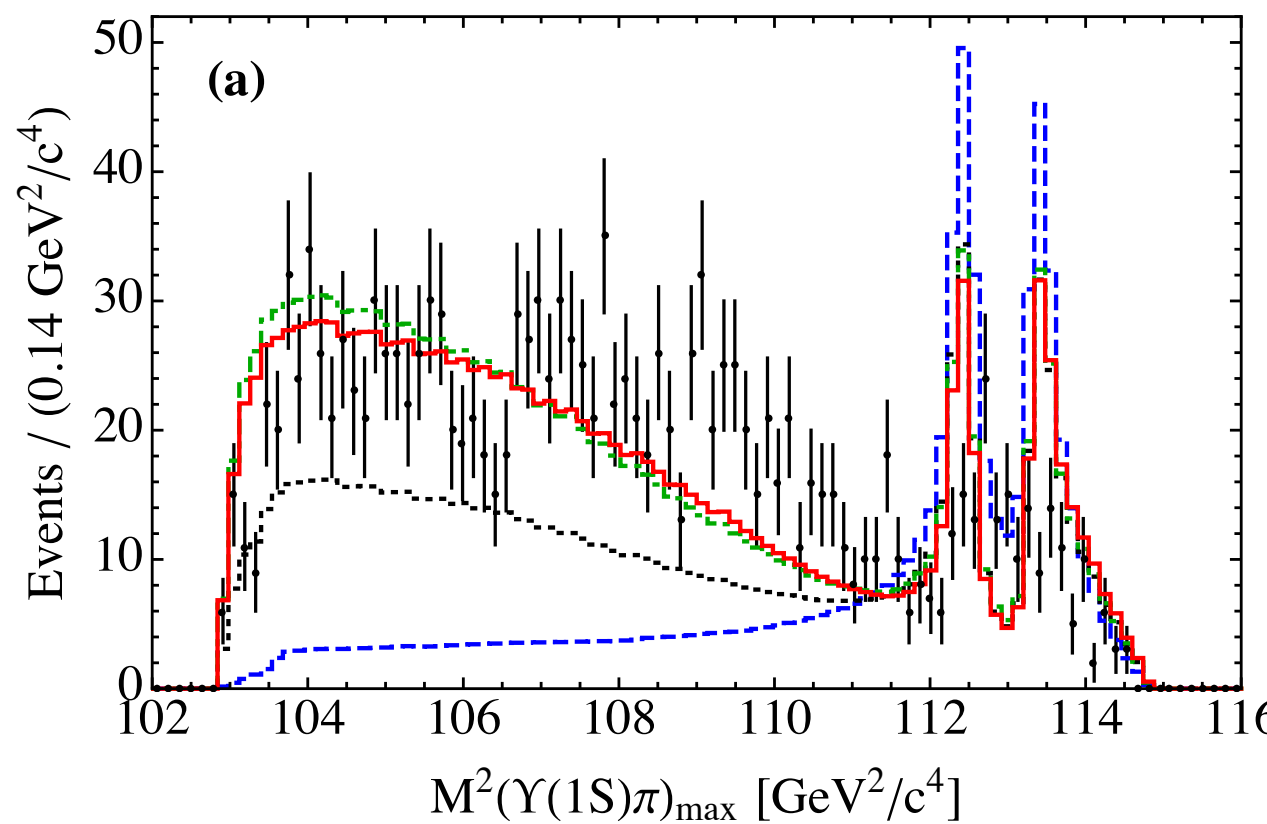
$M^L(t, u) = U(t) + U(u)$ “Z_b”

+ dispersive integral

+ chiral CT's

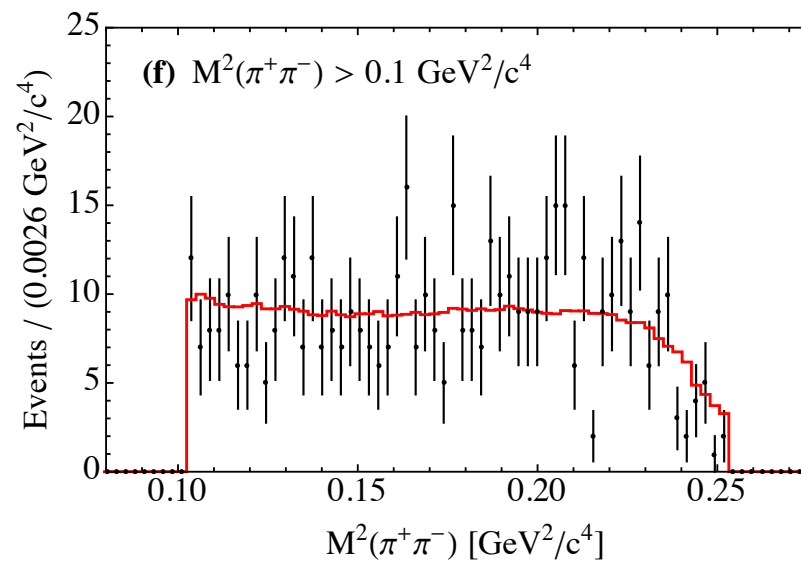
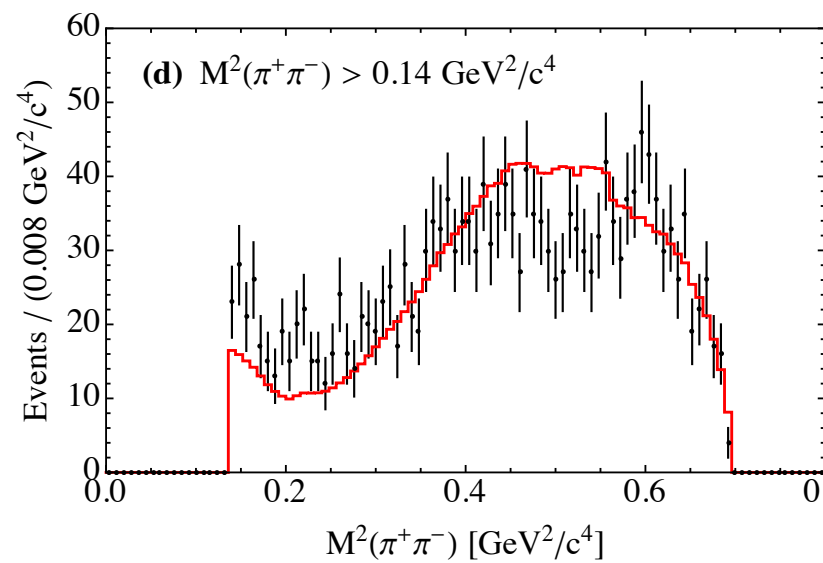
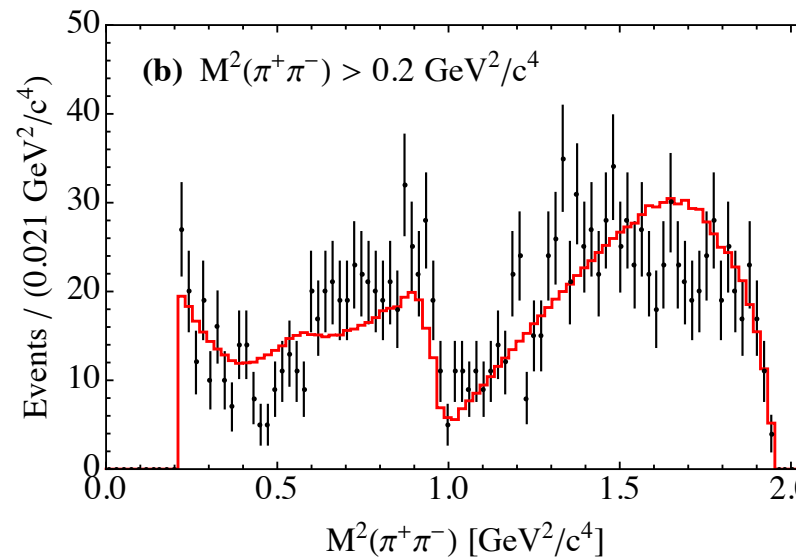
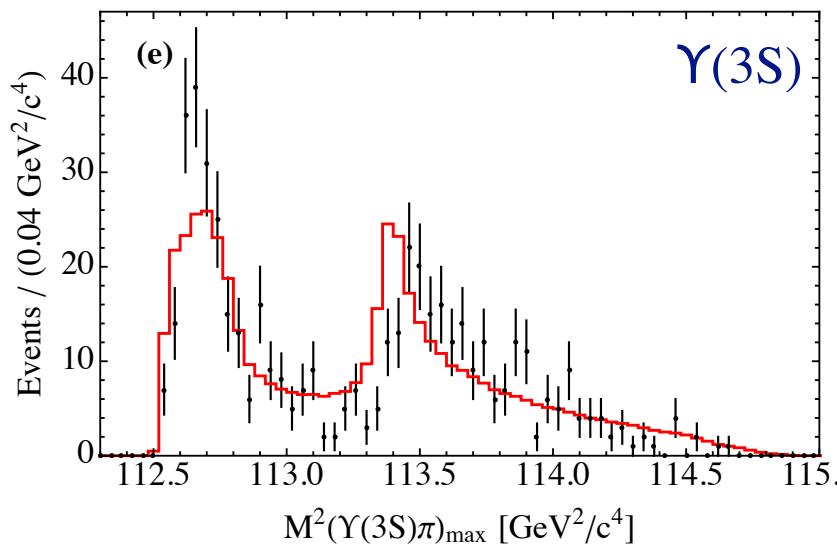
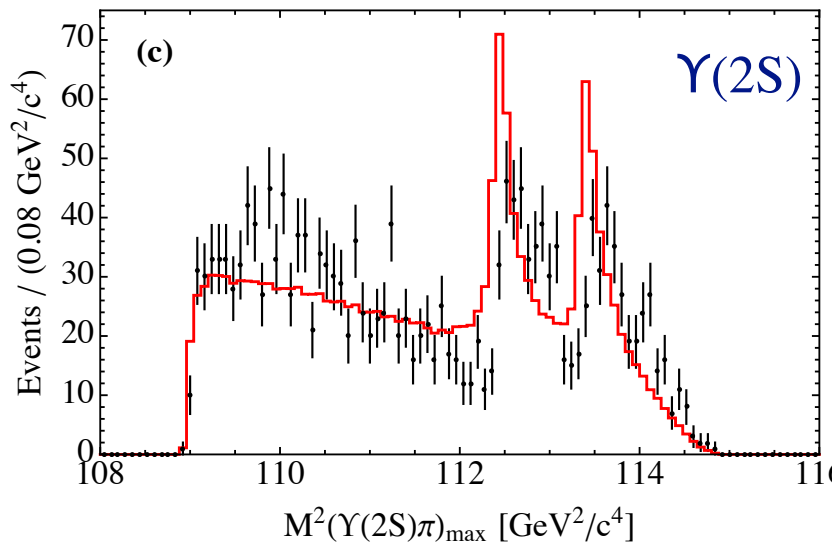
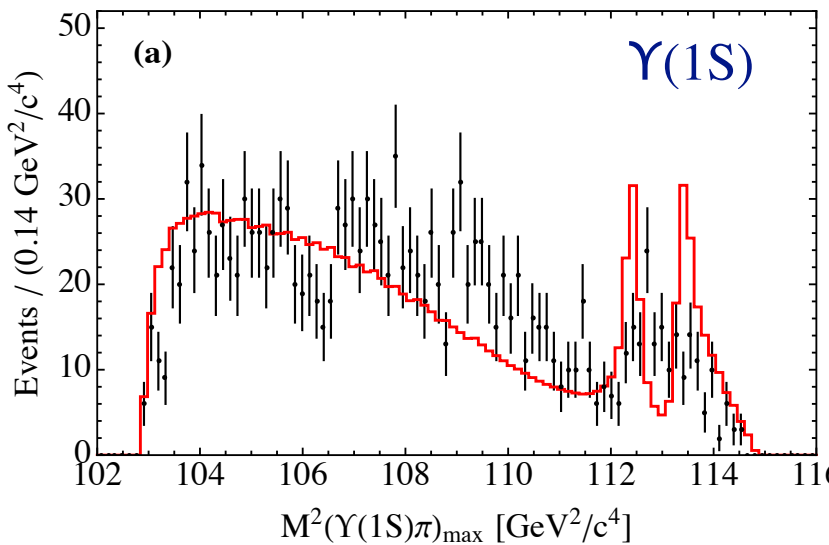
Dalitz plot projections: Individual Contrib's.

$\Upsilon(10860) \rightarrow \Upsilon(1S) \pi^+ \pi^-$



- $M^L(t, u) = U(t) + U(u)$ “Z_b”
- + dispersive integral
- + chiral CT's
- + D-wave $\pi\pi$ FSI

Results for $M(\pi\Upsilon(nS))^2$ and $M(\pi\pi)^2$ projections



$\Upsilon(1S)$ and $\Upsilon(2S)$

► $\pi\pi$ -KK FSI very important

Key contribution to:

— right shoulder in $M(\pi\pi)^2$

— left shoulder in $M(\pi\Upsilon(nS))^2$ $n=1,2$

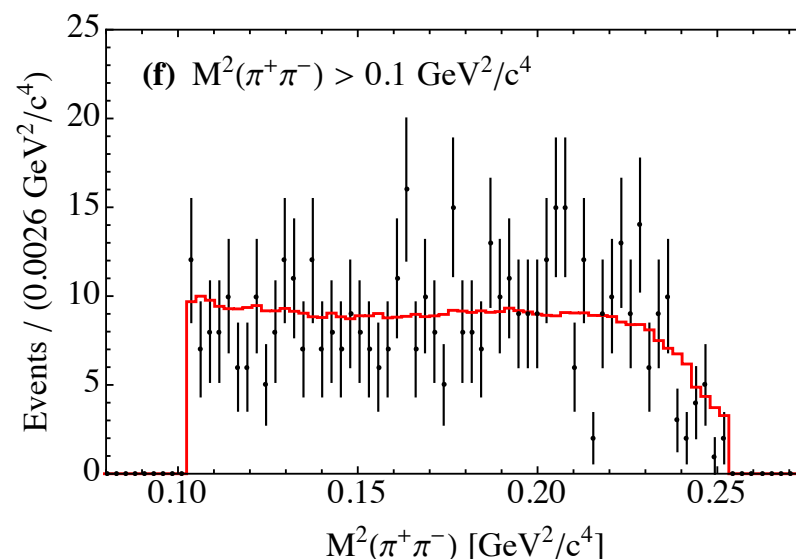
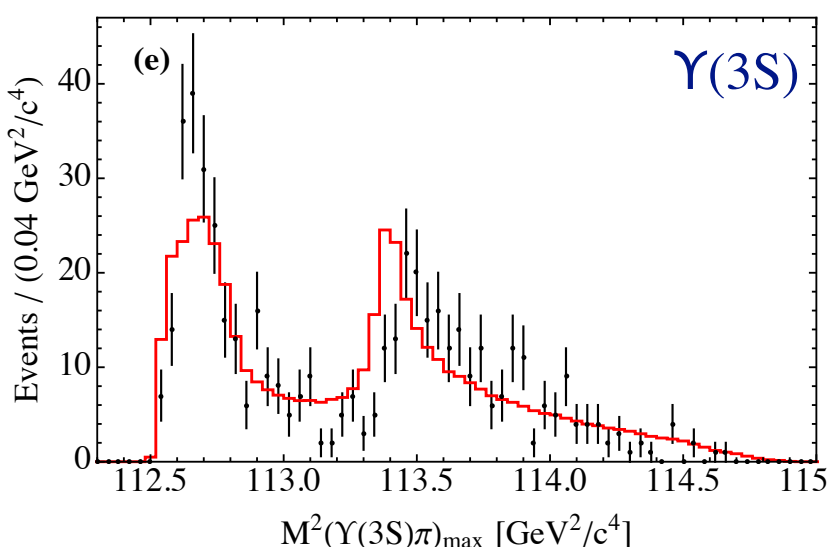
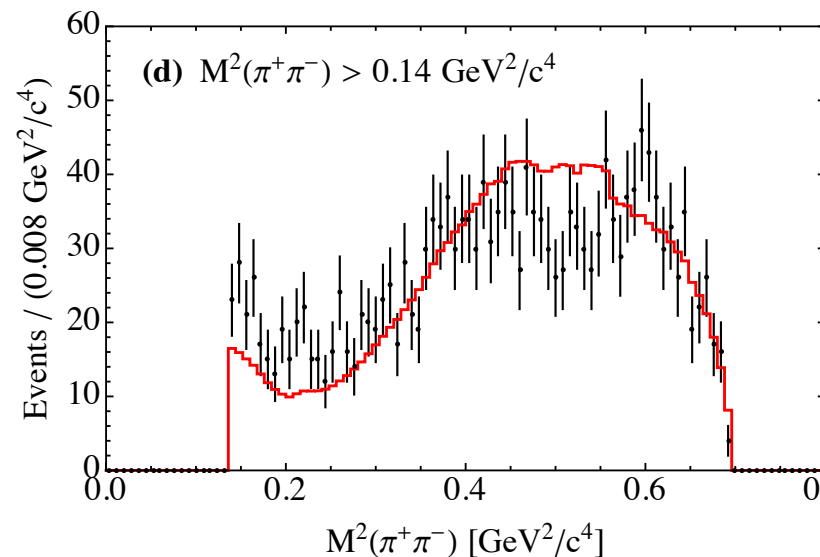
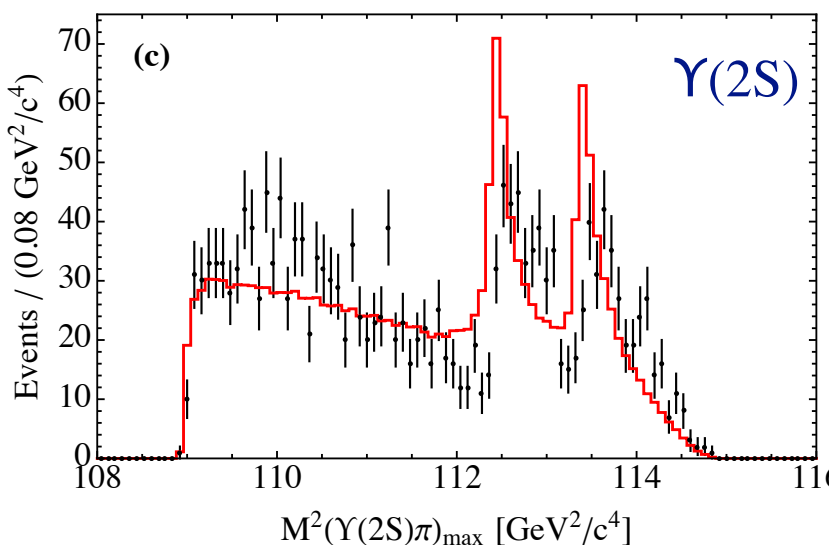
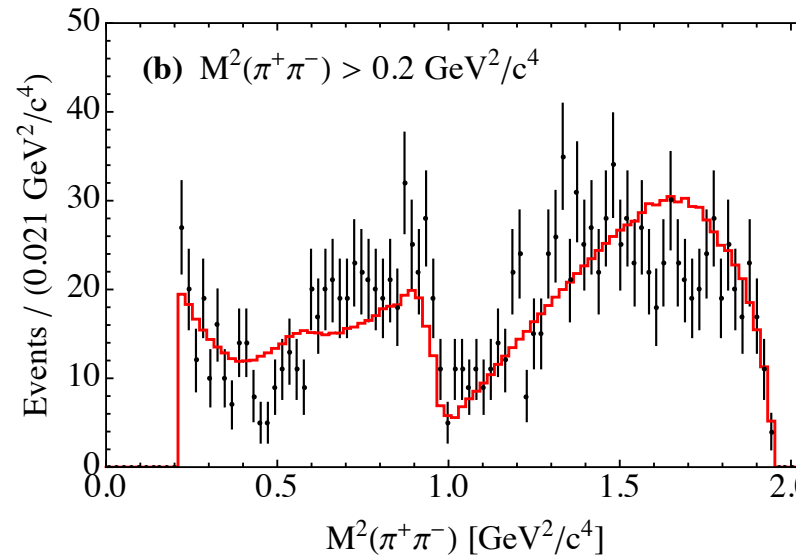
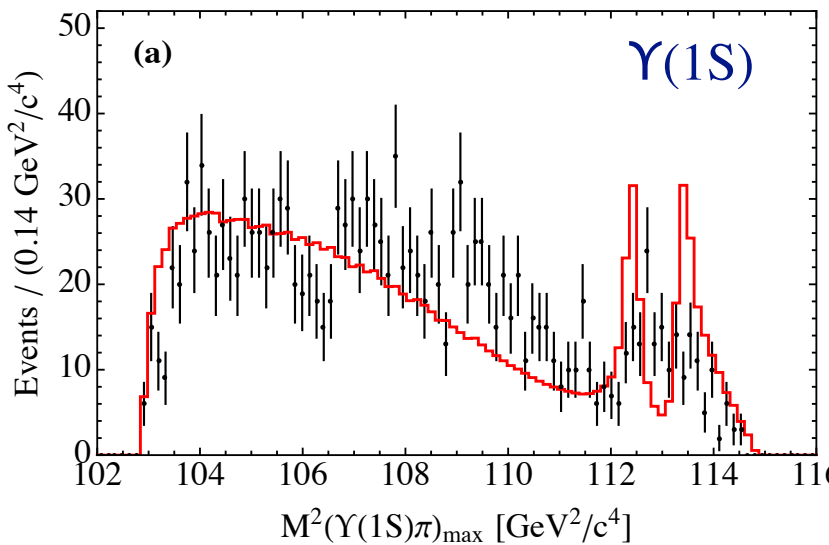
— dip region $\sim 1 \text{ GeV}$ in $M(\pi\pi)^2$

$\Upsilon(3S)$

► Completely dominated by
 $M^L(t,u) = U(t) + U(u)$

► $\pi\pi$ FSI is not important

Results for $M(\pi\Upsilon(nS))^2$ and $M(\pi\pi)^2$ projections



$\Upsilon(1S)$ and $\Upsilon(2S)$

► $\pi\pi$ -KK FSI very important

Key contribution to:

— right shoulder in $M(\pi\pi)^2$

— left shoulder in $M(\pi\Upsilon(nS))^2$ $n=1,2$

— dip region ~ 1 GeV in $M(\pi\pi)^2$

$\Upsilon(3S)$

► Completely dominated by
 $M^L(t,u) = U(t) + U(u)$

► $\pi\pi$ FSI is not important

— Very reasonable overall
description

► Peaks of the Z_b 's, consistent with $B^{(*)}\bar{B}^*$ and $\pi\pi h_b(mP)$, are not exactly in accord with $\pi\Upsilon(nS)$

Summary

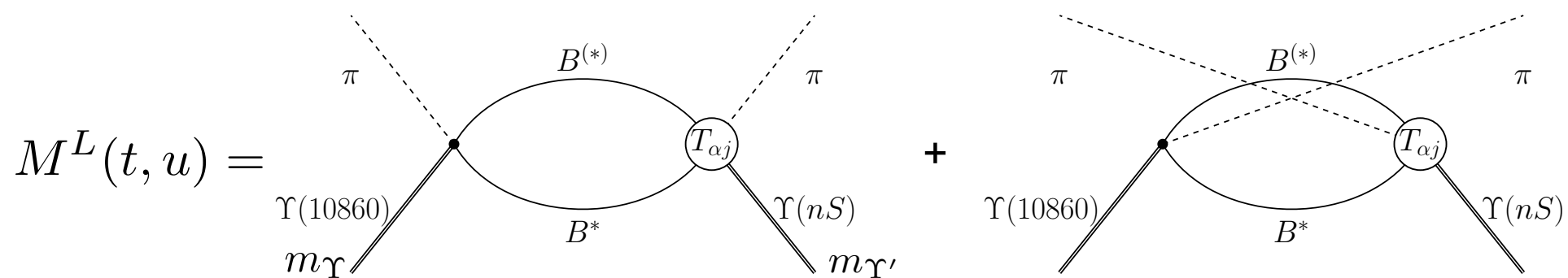
- A chiral EFT based analysis of $\Upsilon(10860) \rightarrow \pi Z_b^{(')} \rightarrow \pi B^{(*)} \bar{B}^* \rightarrow \pi\pi h_b(mP)$
 \Rightarrow poles and residues of the $Z_b(10610)$ and $Z_b(10650)$ are extracted
- An analysis of the Dalitz plots for $\Upsilon(10860) \rightarrow \pi Z_b^{(')} \rightarrow \pi\pi \Upsilon(nS)$
 - The production amplitude w/o $\pi\pi$ FSI is taken from the EFT approach *parameter free*
 - A dispersive approach to deal with crossed channels is employed: the $\pi\pi$ - $K\bar{K}$ FSI is calculated with the minimal number of parameters and Im parts being under control
 \Rightarrow A very reasonable description of the $\pi\pi$ and $\pi\Upsilon$ spectra
serves as a good consistency check for the whole approach

Next steps:

- A dispersive analysis including the OPEP
- A combined analysis of data in all channels within the same framework

Backup

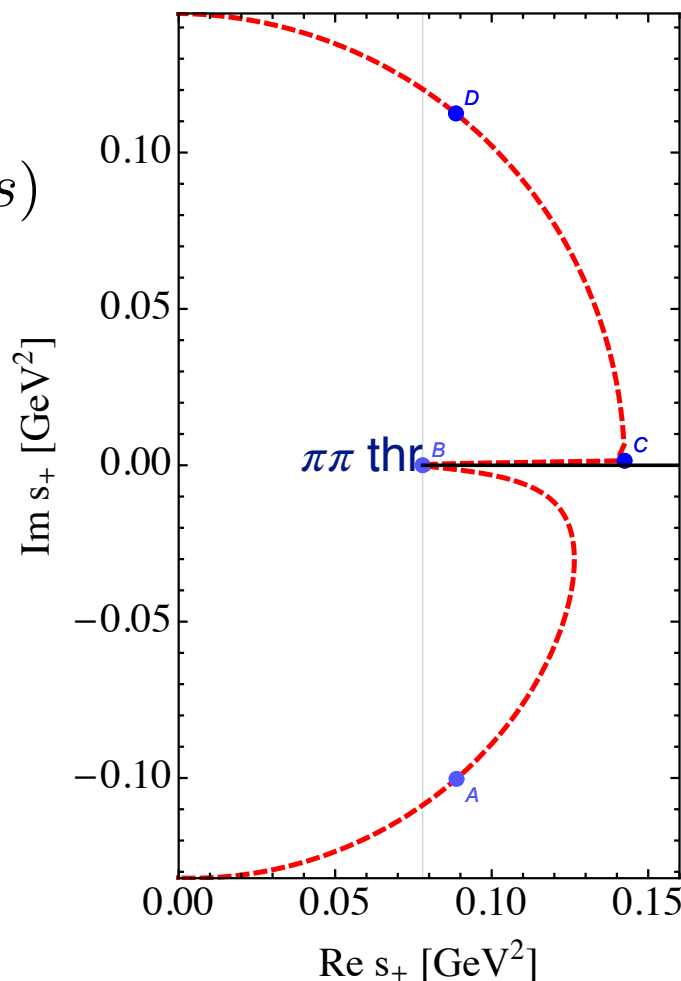
Left-hand cut production amplitude



☞ $Z_b(10610)/Z_b(10650)$ are poles in the coupled-channel amplitudes

$$M^L(t, u) = U(t) + U(u) = -\frac{1}{\pi} \int_{(m_\pi + m_{\Upsilon(1S)})^2}^{\infty} d\mu^2 \operatorname{Im} U(\mu^2) \left(\frac{1}{t - \mu^2} + \frac{1}{u - \mu^2} \right)$$

S-wave
→ $M_0^L(s)$



— Take care about anomalous thresholds = Log branch points of $M_0^L(s)$

$$s_{\pm} = \frac{(m_Y^2 - m_{Y'}^2)^2}{4\mu^2} - \frac{\left(\sqrt{\lambda(m_Y^2, m_\pi^2, \mu^2)} \pm \sqrt{\lambda(m_{Y'}^2, m_\pi^2, \mu^2)} \right)^2}{4\mu^2}$$

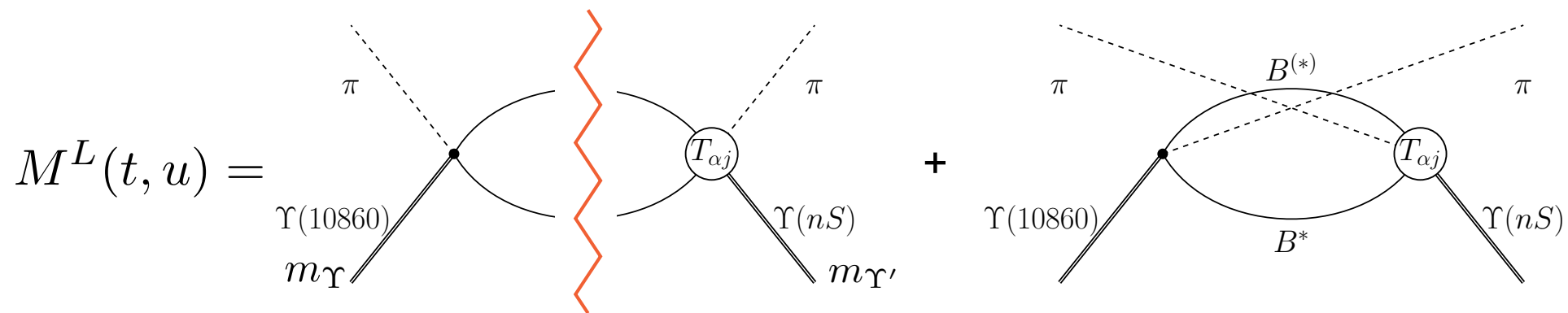
s+ when μ is varied →

☞ s+ hits the $\pi\pi$ threshold and goes to the 1st sheet at the point B if

$$\mu^2 \leq \mu_{\text{crit}}^2 \equiv \frac{1}{2}(m_{\Upsilon(nS)}^2 + m_{\Upsilon(10860)}^2) - m_\pi^2$$

For $\Upsilon(3S)$: $\mu_{\text{crit}} = 10.6097 \text{ GeV}$ very close to $Z_b(10610)$ pole

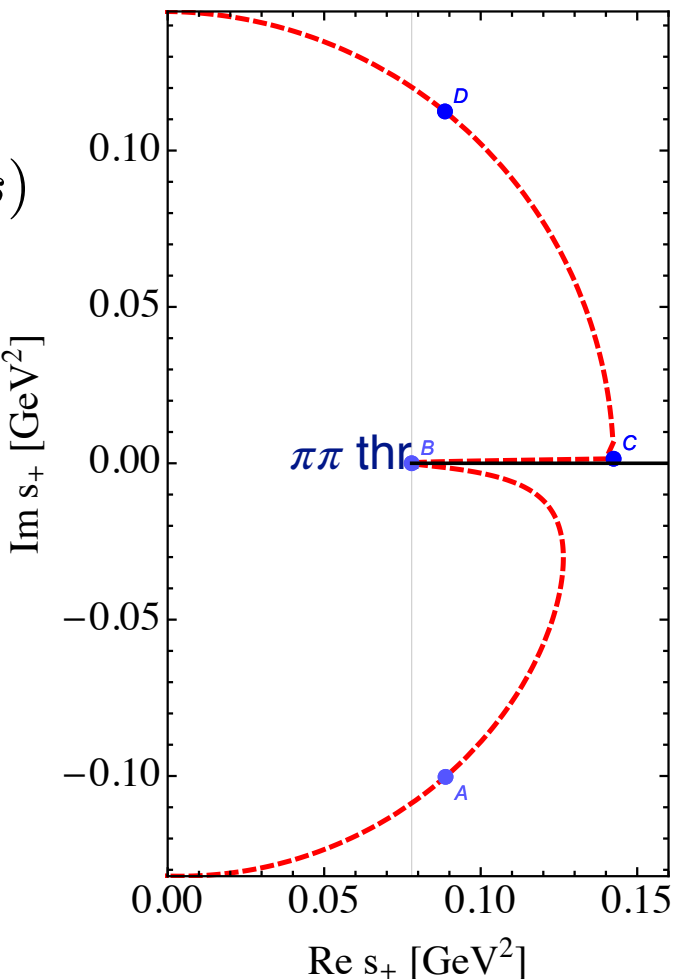
Left-hand cut production amplitude



☞ $Z_b(10610)/Z_b(10650)$ are poles in the coupled-channel amplitudes

$$M^L(t, u) = U(t) + U(u) = -\frac{1}{\pi} \int_{(m_\pi + m_{Y(1S)})^2}^{\infty} d\mu^2 \operatorname{Im} U(\mu^2) \left(\frac{1}{t - \mu^2} + \frac{1}{u - \mu^2} \right)$$

S-wave
→ $M_0^L(s)$



- Take care about anomalous thresholds = Log branch points of $M_0^L(s)$

$$s_{\pm} = \frac{(m_Y^2 - m_{Y'}^2)^2}{4\mu^2} - \frac{\left(\sqrt{\lambda(m_Y^2, m_\pi^2, \mu^2)} \pm \sqrt{\lambda(m_{Y'}^2, m_\pi^2, \mu^2)} \right)^2}{4\mu^2}$$

s+ when μ is varied →

- ☞ s+ hits the $\pi\pi$ threshold and goes to the 1st sheet at the point B if

$$\mu^2 \leq \mu_{\text{crit}}^2 \equiv \frac{1}{2}(m_{Y(nS)}^2 + m_{Y(10860)}^2) - m_\pi^2$$

For $Y(3S)$: $\mu_{\text{crit}} = 10.6097 \text{ GeV}$ very close to $Z_b(10610)$ pole

- $\operatorname{Im} M_0^L(s)$: Leading contribution is from the $B^{(*)}\bar{B}^*$ cuts, these states can be on shell subleading one— from inelastic channels